Central Development Laboratory

NORTH AMERICAN ARC
ALMA Regional Center

NA ALMA Development Cycle 7 Study (2019-2020)
ALMA Band 6 Local Oscillator Modifications

Final Report

22 April 2021

Prepared By Name(s) and Signature(s)	Organization
K. Saini	NRAO
D. Vaselaar	NRAO
M. Mereles	NRAO
Approved By Name(s) and Signature(s)	**Organization**
K. Saini	NRAO
Released By Name(s) and Signature(s)	**Organization**
B. Hawkins Digitally signed by Bert Hawkins Date: 2021.04.26 00:11:19 -04'00'	NRAO

Table of Contents

1 Background and purpose

The receiver noise temperature of the present ALMA Band 6 receiver increases substantially outside of 6 – 10 GHz IF band. Although the accessible IF range has been increased from 5 – 10 GHz to 4.5 – 10 GHz, to allow simultaneous observations of ^{13}CO and ^{12}CO lines, however, doing so places these lines in a very non-optimal region in the receiver IF range.

Of foremost importance is reducing the noise temperature at the edges of the 4 – 12 GHz IF band, particularly on the low frequency side. This will allow the ^{13}CO and ^{12}CO lines at 220.4 GHz and 230.5 GHz to be observed simultaneously with improved sensitivity. This study investigated ways to reduce the AM noise present on the sidebands of the Band 6 Front-end local oscillator in order to improve the overall receiver noise and line sensitivity when using low IF frequencies to observe certain spectral lines.

The amount of “excess” LO noise and the resulting receiver performance degradation were described in detail in the study proposal [RD1] and are not repeated here. The reader is referred to that document for further information in that regard.

2 Description of the Band 6 local oscillator configuration

The following paragraphs provide a brief description of the Band 6 local oscillator system configuration and help to identify the potential problem areas which need to be investigated.

As indicated in Figure 1, the front-end local oscillator hardware is divided between the room-temperature part of the receiver and the cryogenic portion located in the cryostat. Since the final LO frequency can be as high as 265 GHz, therefore to minimize path loss after the final multipliers, the final frequency multipliers are located inside the cryostat as close to the mixers as possible. For power dissipation and volume considerations, the remainder of the first LO is placed outside the cryostat. The room temperature portion of the Front-end LO is housed in the Warm Cartridge Assembly (WCA) and is also sometimes called the first LO “driver”. The Band 6 WCA LO output ranges from 73.7 – 88.3 GHz, which is also quite high in frequency. To minimize loss and phase drift, the WCA output is rigidly attached to the cold cartridge LO waveguide input with blind-mate waveguide flanges and alignment pins. To adequately drive the cold multipliers, the cold cartridge designers had to minimize the RF loss between the WCA and the cold multiplier inputs. To minimize any impedance mismatch induced spectral ripple, caused by standing waves which can potentially degrade the amplitude noise of the LO, the remainder of the first LO components are located close together all inside the WCA housing.

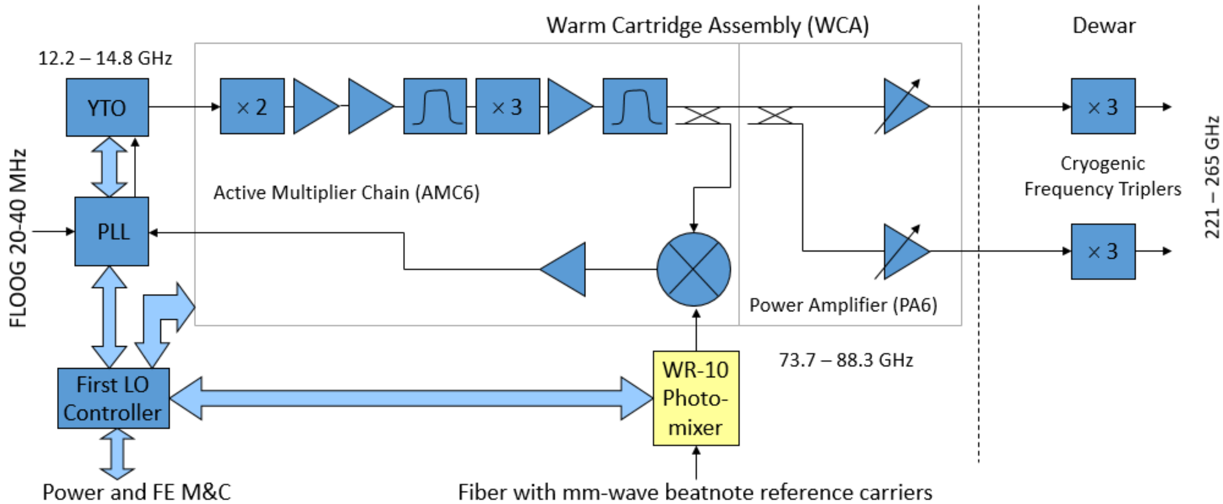

Figure 1: Schematic diagram of the signal flow for the generation of the ALMA Band 6 Front-End Local Oscillator.

The WCA portion of the Band 6 LO consists of three basic modules. The fundamental oscillator, covering 12.2 – 14.8 GHz range, is a YIG tuned oscillator (YTO). The YTO is a commercially available unit and was the only choice during the design phase for broadband electronically tunable VCOs with a low enough phase noise required for ALMA. Following the YTO are two custom blocks, the AMC (Active Multiplier Chain) and the PA (Power Amplifier). The function of the AMC is to frequency-multiply, filter, and amplify the YTO output up to the LO driver frequency of 73.7 – 88.3 GHz. The AMC also performs the function of mixing a sample of this generated LO signal with the millimeter-wave phase reference from the photomixer (which is attached directly to the AMC). The IF output from this AMC mixer is routed to a PLL (Phase Lock Loop) module, which in turn generates the error signal to phase lock the YTO. The PA module splits the AMC output into two channels and independently amplifies the two RF signals. The final RF power level at each PA output is computer controllable to enable optimization of the pumped SIS mixer current at each LO frequency. Short copper-plated stainless-steel waveguide sections are used to connect the PA outputs to the cold cartridge input flange to minimize conductive heat transfer from the PA to the cold cartridge while simultaneously minimizing the RF losses.

It has been observed that the measured LO noise sidebands on the two polarization channels are similar. This leads to the hypothesis that they must be generated in the AMC electronics, prior to the RF splitter in the power amplifier. This is supported by additional experimental evidence, see Figure 2, obtained by measuring the AM side-band noise at the output of the AMC and comparing it with the sideband noise at the output of the AMC and PA combination. The AM noise test set [RD2] requires a constant input power level of 12 mW which the Band 6 AMC is incapable of supplying, consequently, comparing the absolute AM noise values between the two measurements is of limited quantitative significance. However, it can be noted that the relative shape of the AM noise profile of the AMC and PA combination correlates closely with the AM noise profile at the AMC output. Although there is some empirical and test evidence that the saturation level of the power amplifier MMICs have some impact on the level of the eventual side-band AM noise, however, it can be concluded that the noise profile once generated in the AMC is generally preserved.

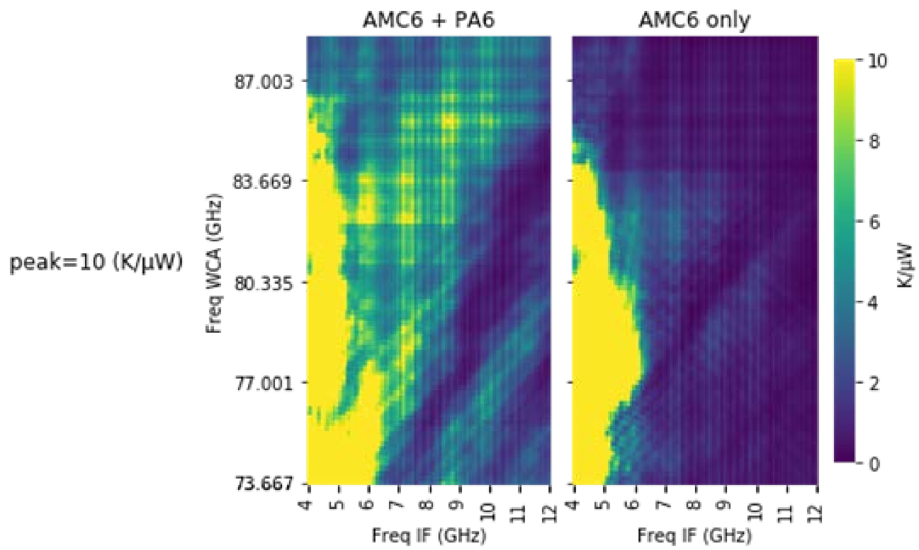

Figure 2: Comparison of AM side-band noise with and without power amplifier.

As shown in Figure 3, the AMC itself consists of a frequency doubler stage, followed by two stages of amplification, a band-pass filter, a frequency tripler, another stage of amplification, and another band-pass filter. The emerging signal is launched into the WR-10 output waveguide.

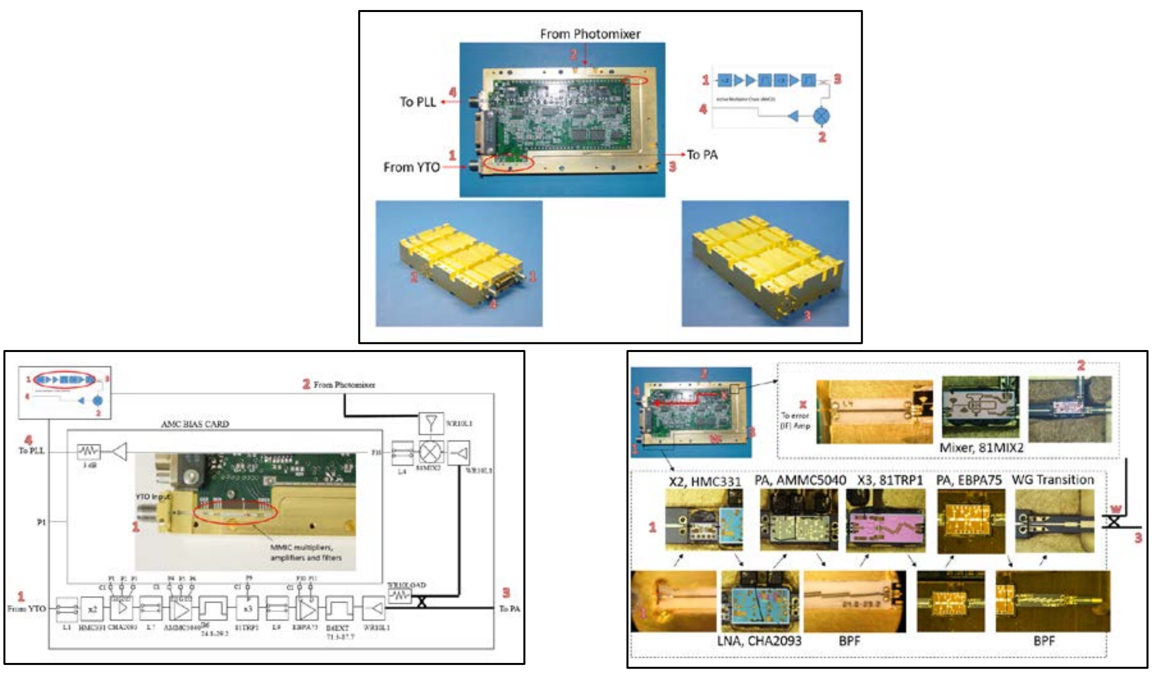

Figure 3: ALMA Band 6 Active Multiplier Chain (AMC6).

3 Scope of the study

The goal of the study was to, initially, fully characterize the performance of the active frequency multiplier (AMC) module's frequency tripler and document its performance – a piece of information that was lacking from the original design/construction phase. Subsequently various modifications to local oscillator modules, as described in the proposal [RD1] and also informed by the AMC frequency tripler characterization, were carried out and the resulting performance was evaluated. A new LO architecture was also prototyped, and evaluated for its AM noise performance. All of the results are summarized in this study report. Additionally, for feasible solutions/approaches that were identified during the course of this study, the cost and effort of upgrading the Band 6 LO system on the ALMA telescope have been worked out and presented along with some preliminary recommendations.

This investigation is a follow-up to the Band 6v2 Conceptual Design Review panel recommendation to improve the LO sideband noise which could potentially enable simplification of the proposed new receiver architecture. Specifically, the Band 6v2 Conceptual Design Review panel in its final report [RD3] recommended to, ". . . investigate the options of using a single-ended mixer (with improvement of the local oscillator noise level) and using a single-ended LNA with isolator. The panel recommends that those investigations are executed to sufficient depth to accurately predict performance and thus provide robust information for the architecture down-selection."

It should be noted that an LO modification/upgrade that improves upon the AM sideband noise, even if implemented in isolation, holds the promise to improve the noise performance of the existing Band 6 receiver.

4 Results of various investigations conducted for the study

The proposal document [RD1] for this study enumerated several tests and experiments to be executed. Most/all of those were carried out and are described below in the same order as they were listed in the proposal. The ensuing results informed additional improvements/test configurations that were also carried out during the course of this study.

4.1 Characterization of the AMC frequency tripler performance

The frequency tripler (81TRP1) used in the AMC, see Figure 5, was previously never characterized. The last recorded measurements made on it were preliminary on-wafer probe-tests done shortly after this custom MMIC was designed back in 2002. New information sought includes: (i.) determining whether the tripler operates at or near the compression levels (or at least in the constant efficiency regime, known to inhibit sideband noise amplification) under the existing drive power and bias conditions; (ii.) if not, whether a higher input power could produce higher output power (this might be useful since more power into subsequent amplifier stages might result in lower AM noise levels further down the signal chain due to amplifier saturation), and; (iii.) absolute maximum permissible input power level, should the existing drive power levels indicate the need for higher input drive power. Presently, it is estimated that the tripler is driven at approximately +20 dBm power level, but there is no information regarding the sensitivity of the output power and/or the resulting AM side-band noise to input power and other operating parameters. It is also unclear if any work was done to optimize the tripler bias. In order to evaluate the tripler and address these questions, tests were performed using the custom block shown in Figure 4, and they are described in the following paragraphs.

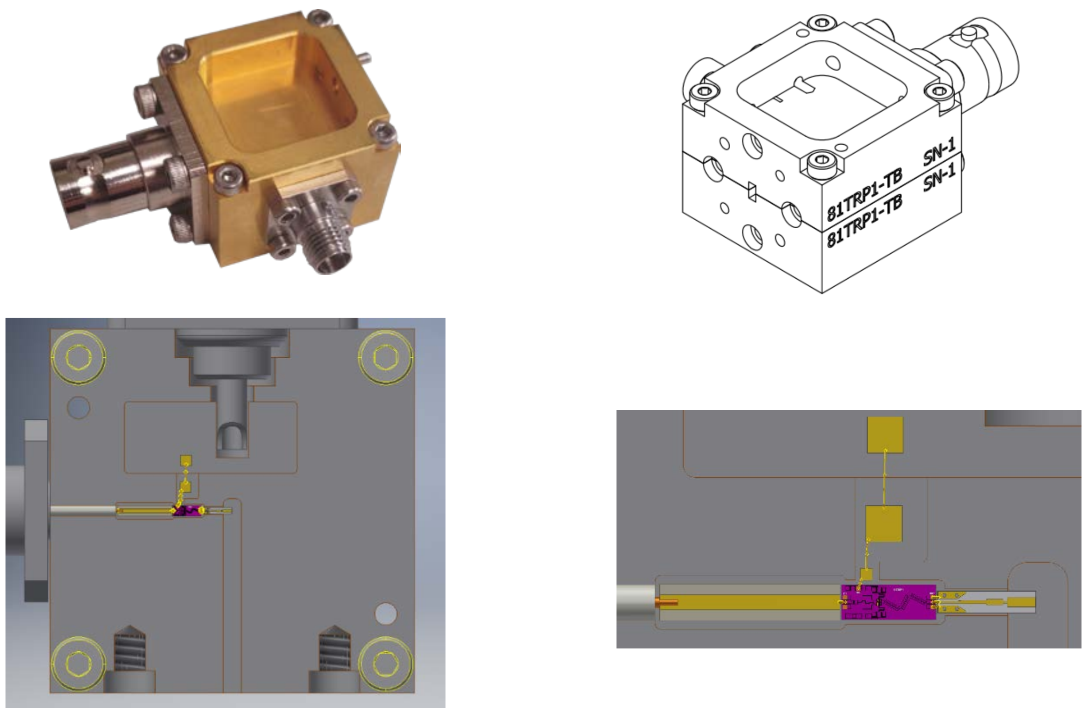

Figure 4: Test block used to evaluate the 81TRP tripler performance. The BNC connector was used to apply a voltage bias to the DUT, an a 2.92mm connection was used for the RF input. The output power of the device was measured via the waveguide output port.

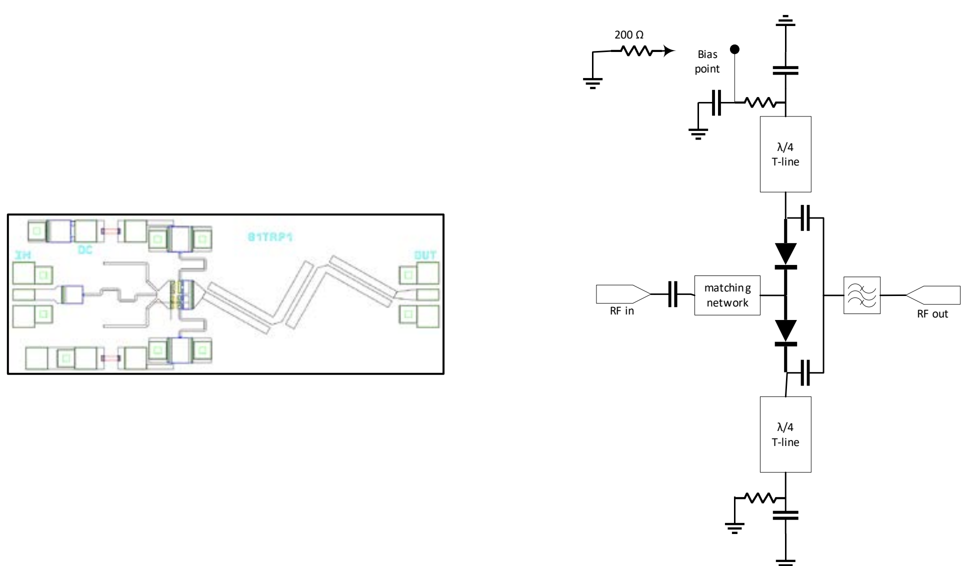

Figure 5: Layout and block-schematic of the 81TRP tripler MMIC.

Figure 6 shows the measured output power/efficiency with the bias port grounded via a 200 Ω resistor. Input frequency was swept from 24 – 30 GHz, and measurements made for input power in the range of 10 – 20 dBm. For the “self-biased” tripler, the output power continues to rise with increasing available drive power levels even though the output efficiency seems to reach a maximum value and begins to show a downward trend for some frequencies.

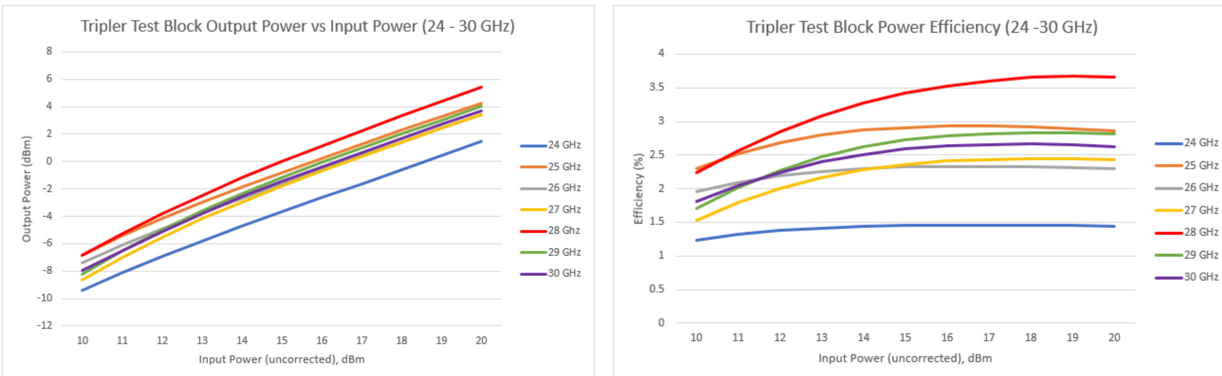

Figure 6: Characterization of the "self-biased" 81TRP1 tripler.

Figure 7 shows the characterization of the tripler output power as a function of input drive power versus the applied voltage at the bias port (instead of the 200 Ω resistor) and input frequency.

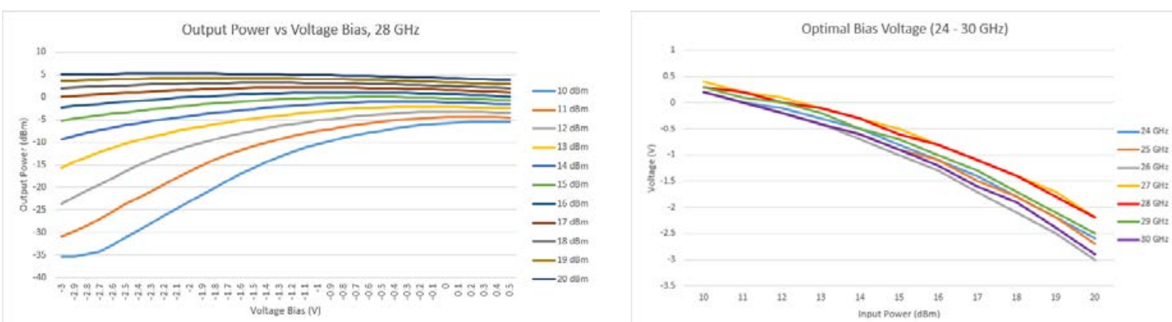

Figure 7: Output power of the 81TRP1 tripler (left) at 28 GHz as a function of input drive level and bias voltage. Similar measurements were made at multiple frequencies (see [RD4]), and although not shown here, the general behaviour at all frequencies is similar. Optimal bias voltage (right) needed to maximize the output power for each input drive level as a function of input frequency.

A dedicated report [RD4] contains a comprehensive description of measurement results from this evaluation campaign. The results shown above are a brief representative summary of the measurements made. These results indicate that for a given input drive power, an optimum bias voltage is required (as a function of frequency) to maximize the output power level, but dramatic change in the output power is unlikely from small deviations in the applied bias voltage, particularly in proximity of the prevailing bias point of ~ 2 V obtained with the self-biasing 200 Ω resistor (which produced a 10 mA measured bias current) in the existing design. Additionally, although the efficiency begins to saturate at 20 dBm input drive level, but still, output power can be increased if the input power is incremented. Therefore, if the generation of the offending sideband AM noise cannot be alleviated by other means, it would be worthwhile to attempt to reduce the LO noise levels by operating this tripler stage with an increased input drive level, thereby saturating the succeeding power amplifier stages to a larger degree. However, doing so would require a higher power driver amplifier with complications of increased DC power requirements, heat dissipation/management, temperature stability etc. With the above complications, and given the lack of sensitivity of the output power to the operating parameters, it was decided to pause this line of investigation, and revisit it later if need be.

4.2 Evaluation of alternative COTS 24-30 GHz amplifiers

The proposal document called for these tests, but the need to do so was contingent upon the outcome of the investigations described in the previous section. If those results implied that the AMC frequency tripler would benefit significantly from a larger drive power (and that 81TRP1 MMIC could handle it), alternative commercial off-the-shelf (COTS) devices could be evaluated by replacing the existing AMMC-5040 amplifier MMIC stage. However, as explained earlier, given the conclusion that the tripler MMIC is already operating close to efficiency saturation, and concerns associated with the use of a higher saturation power amplifier described earlier, this line of investigation was de-prioritized and ultimately not pursued in light of results from other lines of investigation.

4.3 Evaluation of sensitivity to location of 24.8 – 29.2 GHz filter

4.3.1 Motivation for this evaluation

The plot in Figure 8 shows the IDB and MD monitored-current values for the existing AMC6 design. The IDB monitor represents the drain current of the power amplifier that drives the frequency tripler in the AMC, while the MD monitor represents the rectified DC current in the frequency tripler and is indicative of its pump/drive level. The two traces exhibit periodicity (and correlation), which indicates a standing wave between the tripler and the preceding RF amplifier stage, perhaps impacting the latter's performance. The mismatch distance formula, $\Delta l = c/2\Delta f$, indicates that the observed periodicity corresponds to the output signal from the AMMC-5040 tripler leaking back toward the driver amplifier, with the length of the intervening bandpass filter in between. Simulations, see Figure 9, indicate that the bandpass filter has very low isolation/insertion loss at this frequency, so such an interaction is possible.

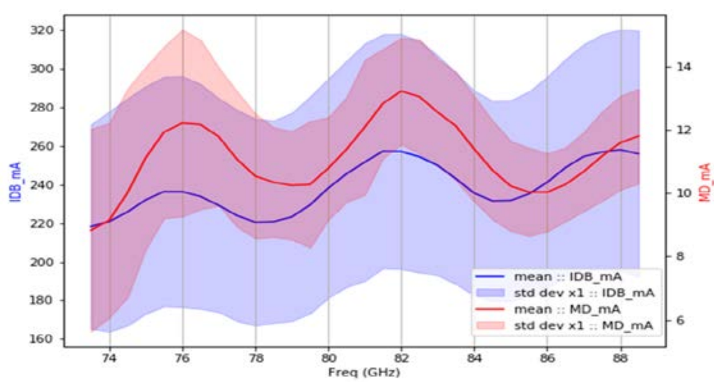

Figure 8: AMC6 IDB and MD monitored-current values. The IDB monitor represents the drain current of the power amplifier that drives the frequency tripler in the AMC, while the MD monitor represents the rectified DC current in the frequency tripler and is indicative of its pump/drive level. There is a large degree of correlation between the peaks and valleys of these two monitor points. Given the correlation of two of these valleys (around 74 and 79 GHz) with the locations of the AM noise spikes, further investigation of the cause of this interaction in warranted. Note that the valley at around 86 GHz represents a higher absolute drive level compared to other two valleys and, perhaps for that reason, it does not correspond to an observed AM side-band noise peak.

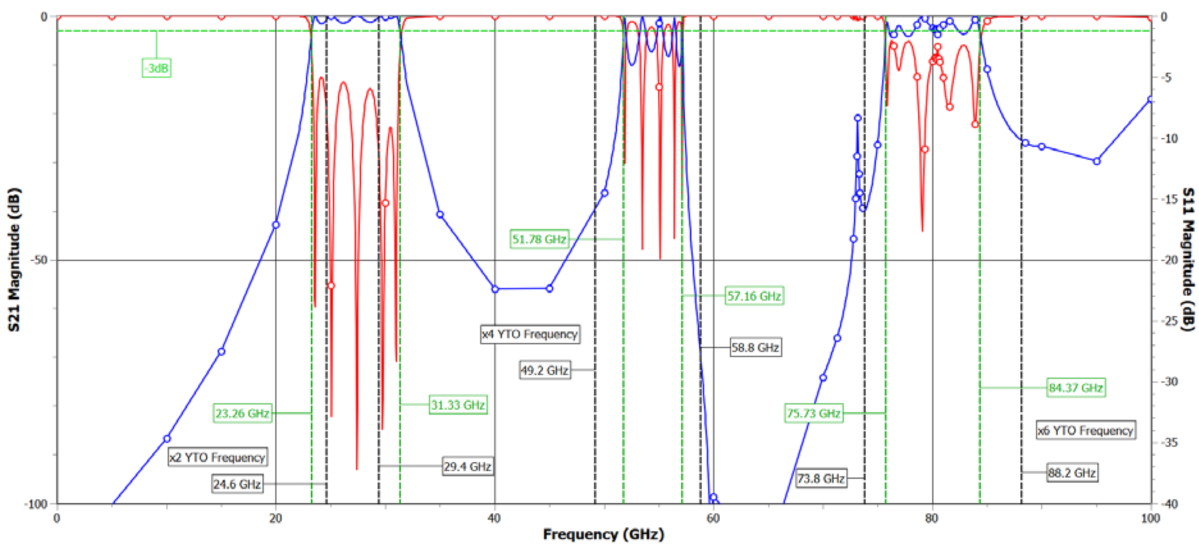

Figure 9: Simulated performance of the 24.8 – 29.2 GHz filter, showing that it has spurious passbands at ×4 and ×6 of the YTO frequency. The latter corresponds to the output frequency range of the tripler and that signal could leak back through this filter.

To reduce the passband amplitude variation from this standing wave, it was proposed to evaluate a modified AMC in which the AMMC-5040 amplifier is moved closer to the tripler, with the intervening bandpass filter moved ahead of the AMMC-5040 amplifier. The bandpass filter could be relocated between the two amplifier stages following the doubler (see Figure 10 and Figure 12) and would still be able to adequately serve its purpose. Minimizing the distance between the mismatched sections could help “stretch out” the spectral ripple thereby reducing the magnitude of variation in the frequency range of interest and perhaps result in sideband AM noise improvement, if this were to be the root cause of the problem.

4.3.2 Reference measurement on a standard configuration AMC6

Figure 10 shows the layout of components in a standard AMC6 configuration. An AMC of this type (AMC6-901) was assembled and tested to record its reference performance for subsequent comparison with the performance of other AMC variants.

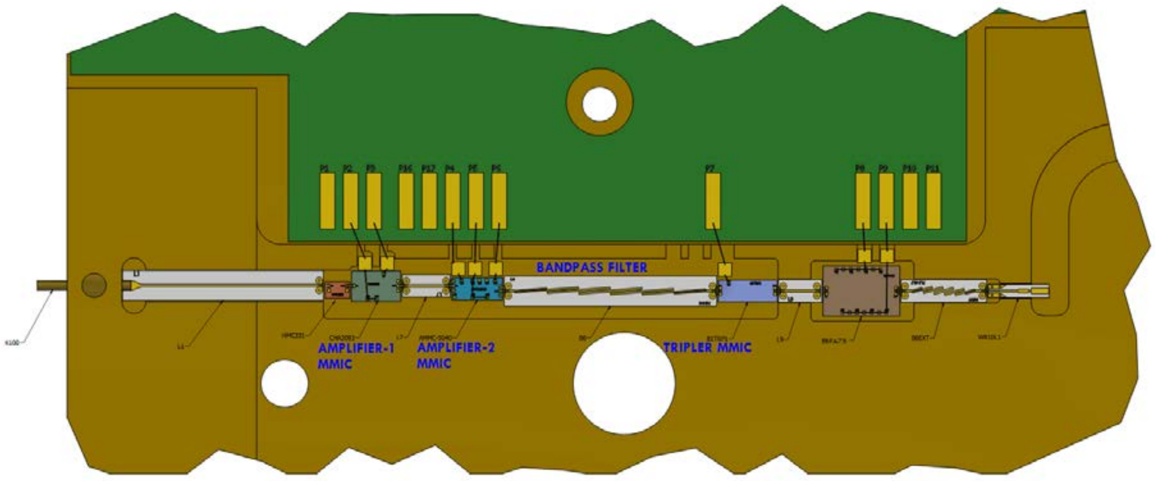

Figure 10: Rendering of a standard AMC6 showing the layout of various components.

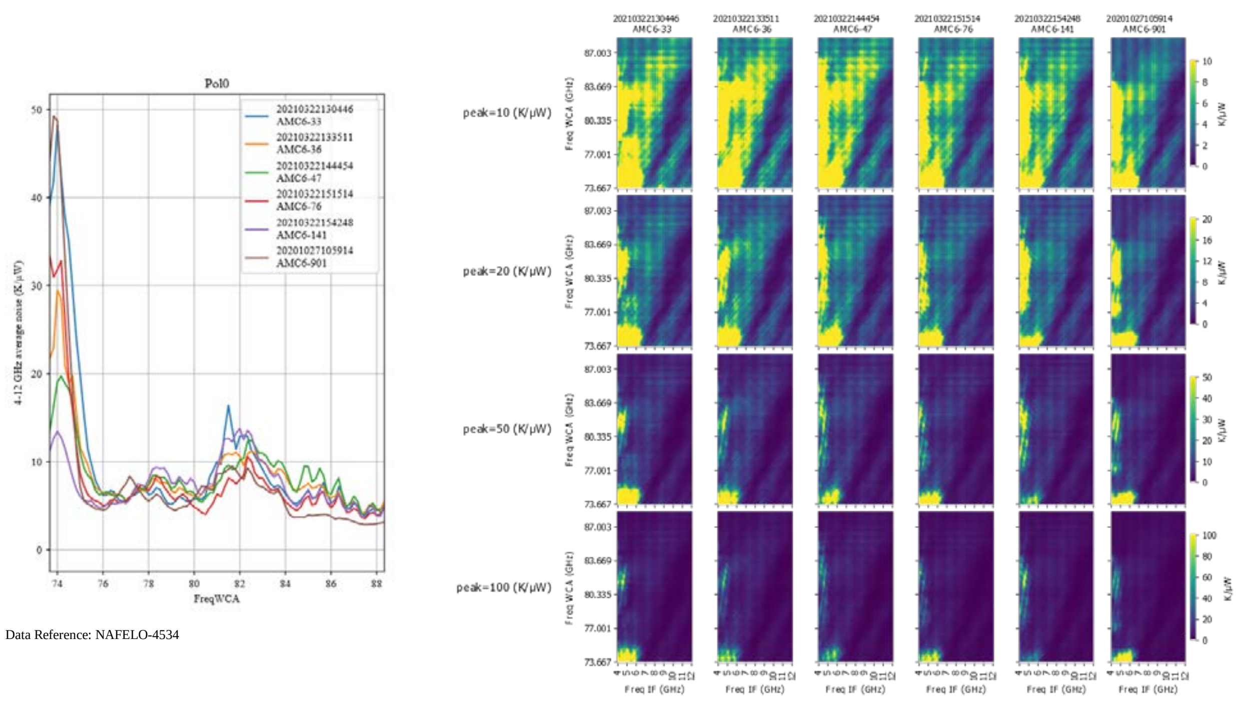

Data Reference: NAFELO-4534

Figure 11: (Left) Averaged (over 4-12 GHz offset from the carrier) AM sideband noise of several standard AMC6 articles, including AMC6-901. (Right) Variously scaled heatmap data, showing the same noise data in terms of spectral components at 4 – 12 GHz offsets from the carrier as a function of LO frequency. AMC6-901 was constructed for the purpose of this study, while the other AMCs are spare Band 6 articles, included here to show that there is some spread in their noise performances. AMC6-901 is one of the poorer performing AMC6s (noise-wise). However, all AMC6s have the same general characteristics and exhibit noise at lower IF offsets from the carrier. ALMA specification is 10 K/µW (applicable to the averaged metric of the left panel in the figure).

4.3.3 Modified AMC (amplifier moved closer to the tripler)

Figure 12 shows the layout of components in a modified AMC where the second amplifier was moved up closer to the tripler as described in the previous section.

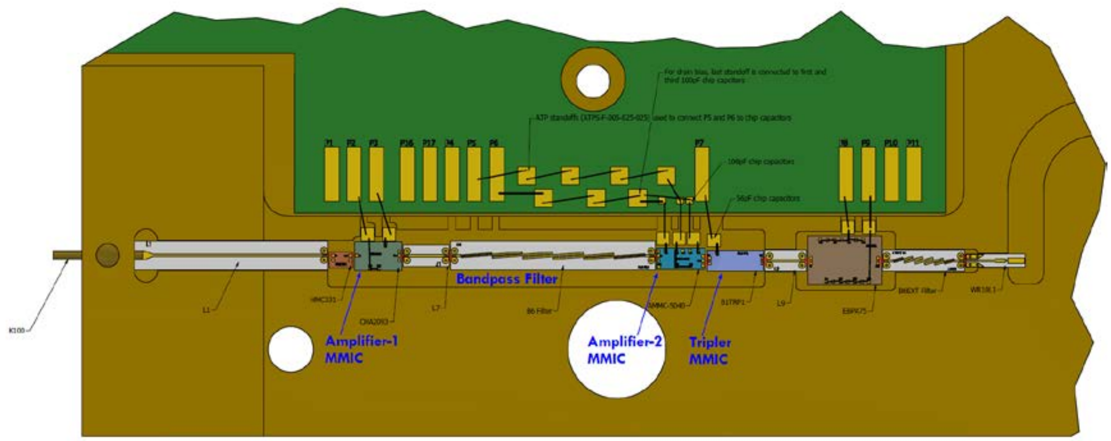

Figure 12: Rendering of a modified AMC6 in which the AMMC-5040 amplifier is moved closer to the tripler, with the intervening bandpass filter moved ahead of the AMMC-5040 amplifier.

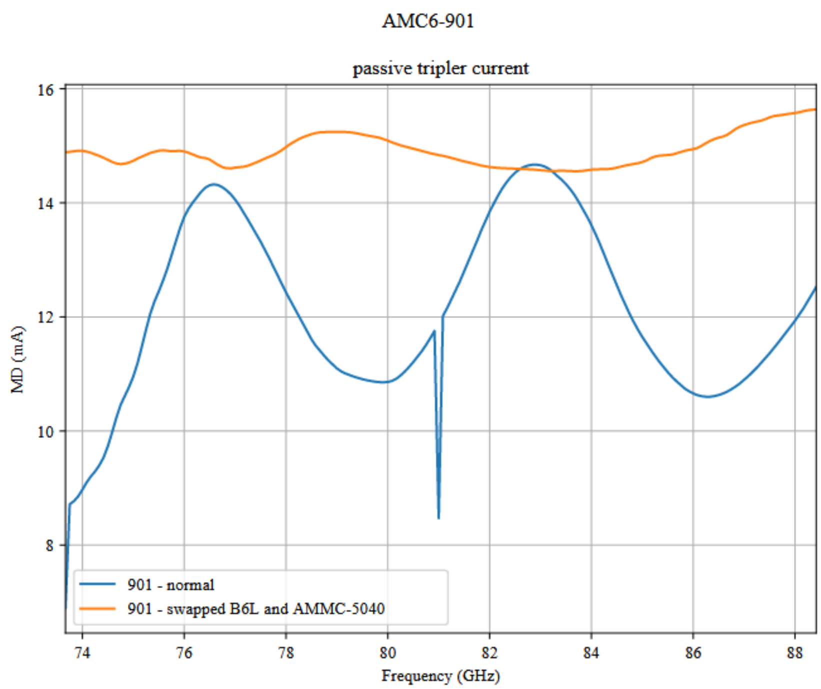

Data Reference: NAFELO-4534 and NAFELO-4563

Figure 13: Measurements of the monitor current (MD) in the passive tripler (81TRP1) – the ripple vs frequency in the monitor current that is seen in the standard AMC6 configuration disappears in the modified configuration with the locations of the second amplifier and the filter swapped. It was hypothesized that the ripple seen in the standard AMC6 was due to the ×3 multiplied frequency component of the tripler leaking out back from its input and creating a standing wave between the AMMC-5040 output and 81TRP1 input through the length of the intervening filter. These results appear to confirm the hypothesis.

The measurement shown in Figure 13 illustrates that minimizing the distance between the second amplifier and the passive tripler sections alleviated the magnitude of pump level variation in the frequency range of interest which seems to support the belief that the standing wave was caused by the leakage of the output frequency of the tripler, back into the amplifier on the input side through the intervening filter length. However, as shown next in Figure 14 and Figure 15, this improvement in the pump levels of the tripler failed to result in an improvement in terms of the AM noise sidebands of the LO signal. A possible reason/conclusion is that the AM sideband noise is likely not being generated in this section of the AMC electronics, although it could perhaps be magnified by the prevailing operating conditions at this stage. Additionally, any "out of band" AM sideband noise generated in the amplifier that might have been filtered by the intervening filter in the original configuration, likely passes through into the tripler in the new configuration, resulting in a degraded AM sideband noise performance.

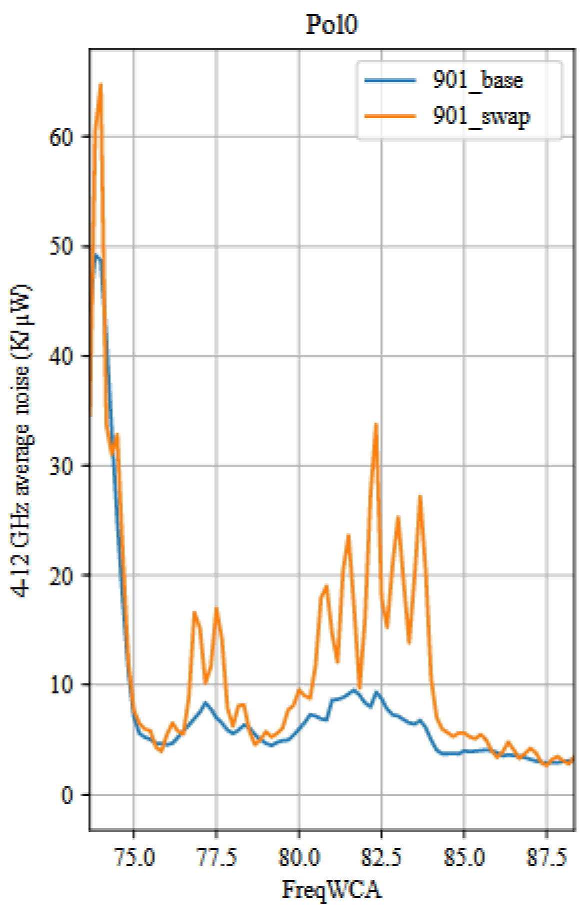

Data Reference: NAFELO-4534 and NAFELO-4563

Figure 14: Comparison of the averaged (over 4-12 GHz offset from the carrier) AM sideband noise of a standard AMC6 versus that of the modified version of Figure 12.

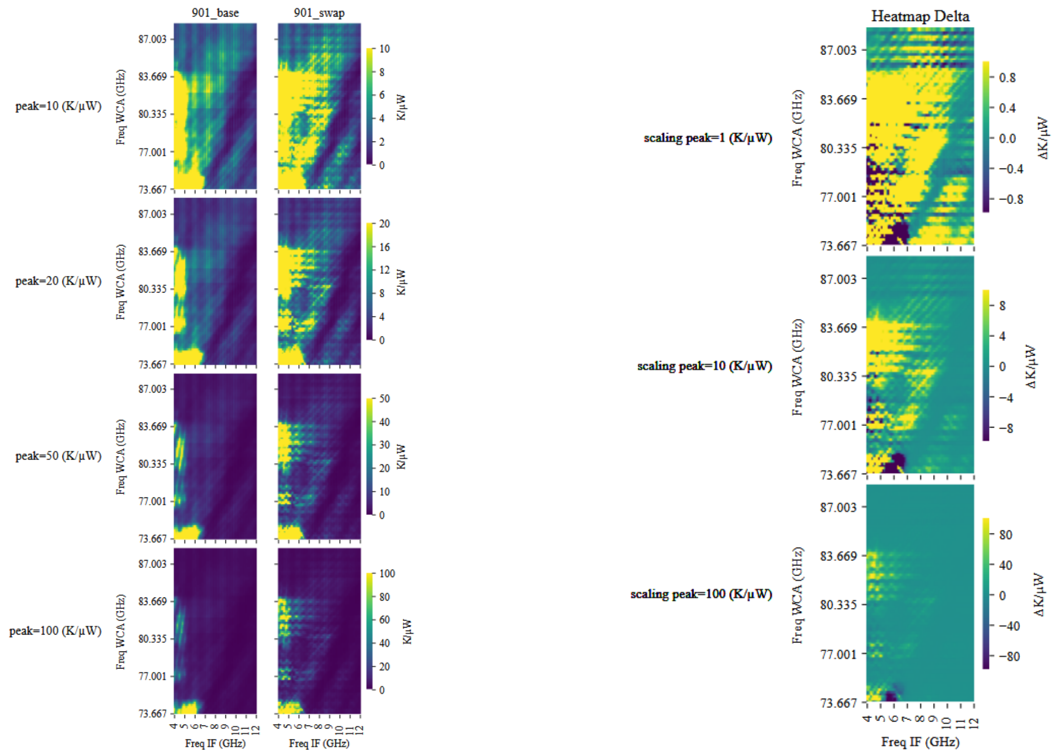

Data Reference: NAFELO-4534 and NAFELO-4563

Figure 15: (Left) Variously scaled heatmaps of the AM sideband noise at 4 – 12 GHz offsets from the carrier as a function of LO frequency. (Right) Delta comparison of the heatmaps. Yellow areas indicate places where the modified configuration has more AM noise, and blue where the noise is less. Turquoise corresponds to no change.

4.4 Evaluation of alternative AMC architectures

Several candidate variations of AMC architectures were listed in the proposal document for evaluation. In addition to those, a few other possibilities were identified during the course of this study. All of them are listed and briefly discussed below in order to identify promising alternatives for further evaluation.

Based on the test results described in the earlier sections, a conclusion is that the root cause of the AM sideband noise generation is most likely not associated with the tripler stage of the AMC6, although the tripler might have some impact on the eventual magnitude of this noise. Consequently, the focus was shifted to investigating noise generation ahead of this stage and close to the input side of the AMC6.

1. Evaluation of an alternate doubler stage: The current design uses Analog Devices HMC331 [RD5] as the input doubler stage. In addition to the fact that this is now an obsolete device (although we have sufficient quantities in stock to maintain the existing AMC6s in the field), this device has a particularly poor input return loss in the 12.2 – 14.8 GHz frequency range, with the worst return loss performance (< 5 dB) at the lowest end of this frequency range which corresponds to the LO frequency where significant AM noise sideband problems are located.

Analog Devices HMC331

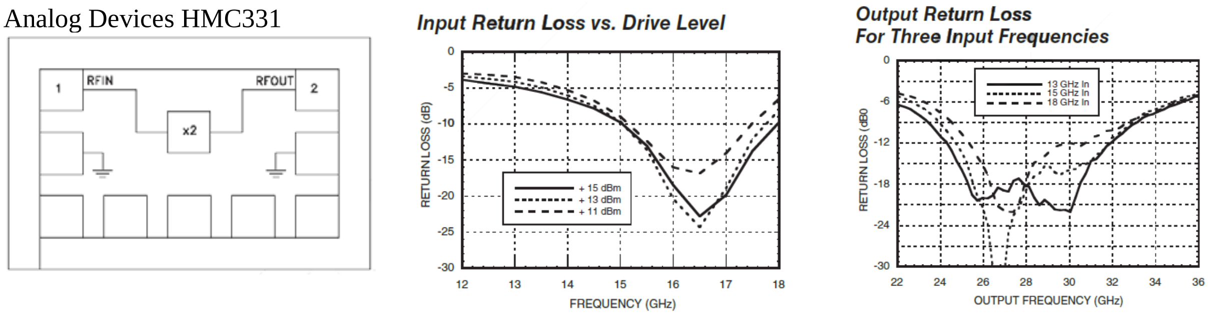

Figure 16: Return loss performance of the Analog Devices HMC331 doubler used in the existing AMC6 design (from datasheet).

An alternate doubler, Analog Devices HMC578 [RD6], has better input return loss over the problem frequency range, although it is comparatively slightly poorer at the upper end of the desired YTO frequency span of 12.2 – 14.8 GHz. Since this device incorporates input and output amplifiers, the AMC configuration would need to be modified to reduce an equivalent amount of gain at an appropriate place elsewhere in the AMC signal chain. Despite this added complication, the possibility of reducing the standing noise waves at the input due to a better input match was considered promising enough and this AMC scheme was selected for further evaluation.

Analog Devices HMC578

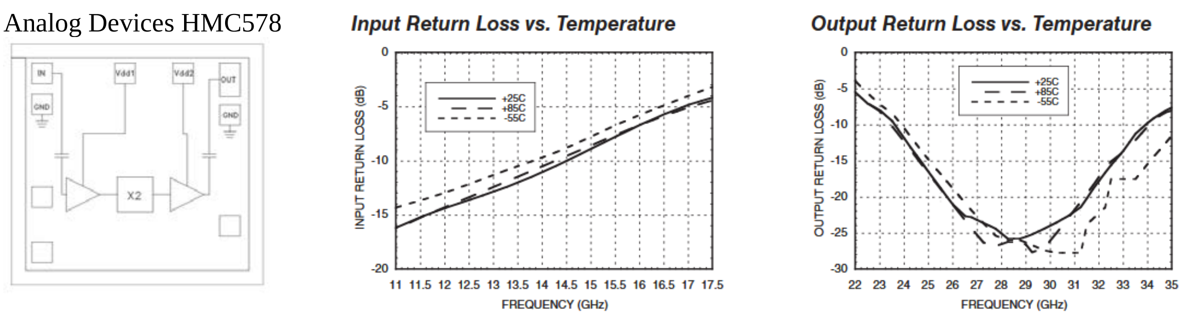

Figure 17: Return loss performance of an alternate Analog Devices HMC578 doubler (from datasheet).

2. Evaluation of a "×2" frequency multiplication scheme: A "×2" multiplication scheme for 73 – 88 GHz output would require a source oscillator frequency range of approximately 36 – 45 GHz. The highest frequency COTS YIG oscillators currently available reach 40 GHz, although some custom devices up to 44 GHz are also advertised. However, these are not expected to be cost effective, and in some cases they incorporate a lower frequency oscillator followed by a discrete doubler stage. Use of such a doubled source for this application is ruled out, since lack of close integration of the multiplier and amplifier stages is known to cause poorer noise performance. Mismatches coupled with long inter-stage lines result in standing waves and unmanageable spectral power dips. At the spectral-dip frequencies, the signal-to-noise level at the subsequent amplifier input can be low enough such that it is significantly degraded by the noise of that amplifier. Standing waves result in the opportunity for enhancement of sideband noise levels since the frequency conversion efficiency can vary greatly at the sideband frequency versus the signal frequency. Consequently, even though the necessary COTS frequency doublers are available (e.g. HMC1105 from Analog Devices) for the desired frequency range, a "×2" multiplication scheme was not considered to be an attractive approach and was consequently not pursued.
3. Evaluation of a "×3" frequency multiplication scheme: An AMC with a "×3" multiplication factor scheme would help confirm the hypothesis that the input "×2" stage and the devices in its immediate

vicinity are indeed the root cause of the AM sideband noise generation. One of the current Band 6 AMC blocks could have all the first-stage “×2” multiplication components removed (Analog Devices HMC331 and UMS CHA2093) and replaced with a through transmission line to bridge the gap. Since the input to such an AMC would be in the 24 – 30 GHz range, the input coaxial-to-microstrip transition would need to be re-optimized to cover the extended frequency range in order to avoid any performance degradation due to mismatches between the YTO and the AMC block input. Another advantage of such an AMC architecture would be that it would place the lowest frequency of the YTO above 20 GHz, which is nominally the extended IF frequency range identified as an ALMA2030 roadmap [RD7] goal in the ALMA FE & digitizer workgroup report [RD8]. Given all of the potential benefits of this approach, the “×3” architecture was selected as a candidate for further evaluation.

4. Based on the study results/findings up to this point, the final W-Band amplifier (custom BAE EBPA75) in the AMC6 was not suspected to be the root cause of the noise issue. The available alternatives like the custom BAE EBPA96B, NG APH667, and NG APH669 could at best help to suppress the previously generated noise sidebands. Since it would be best to avoid their generation in the first place, this line of investigation was not pursued.

4.4.1 Modified AMC with alternate doubler stage (HMC578)

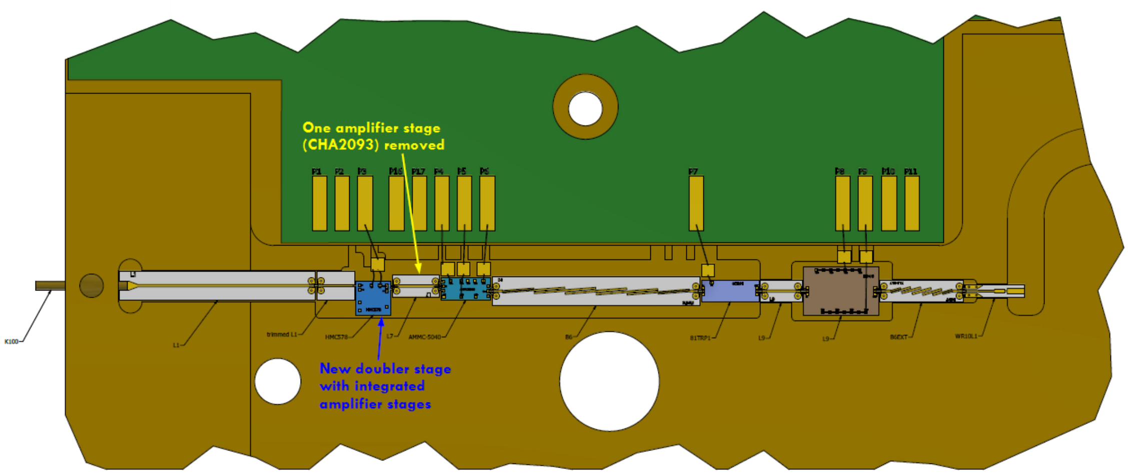

Figure 18: Modified AMC with the Analog Devices HMC578 doubler MMIC (incorporating integrated amplifiers).

The Analog Devices HMC331 doubler has a conversion loss of 14 dB, and in the original AMC6 design, it is followed by a 15 dB gain UMS CHA2093 amplifier with a saturated output power (P_{1dB}) of about 13 dBm. With an input of 17 dBm from the YTO, and after allowing some loss in the input transition of the AMC6, the original design ensured that UMS CHA2093 operated close to saturation and output ~ 14 dBm into the successive stage in the AMC6.

The Analog Devices HMC578 in the modified AMC design, has a saturated output of approximately 17 dBm, allowing for the removal of the UMS CHA2093 amplification stage and thereby closely preserving the operating point for the successive stage in the AMC.

The AM sideband noise performance of this modified AMC was measured and Figure 19 provides a comparison of the results to that of a standard AMC6 performance. The large amount of AM sideband noise present at 4 – 6 GHz offset from the LO carrier at 73.7 GHz in the original design (primary non-compliance with the average noise specification of 10 K/μW) is significantly reduced, while the noise near 82 GHz LO (already compliant with the average noise specification for the original AMC6 design), remains about the same in the case of the alternate design.

The above results support the hypothesis that the poor input return loss of the original doubler component used in the AMC6 design, and the resulting input mismatch, leads to generation of the noise sidebands and poor AM noise performance. The otherwise usual symptoms of spectral output power variations (resulting from the standing wave due to the input mismatch) are not explicitly manifest, perhaps due to the saturated operation of several amplifier stages in the AMC6 design, which likely mutes that effect to a large extent.

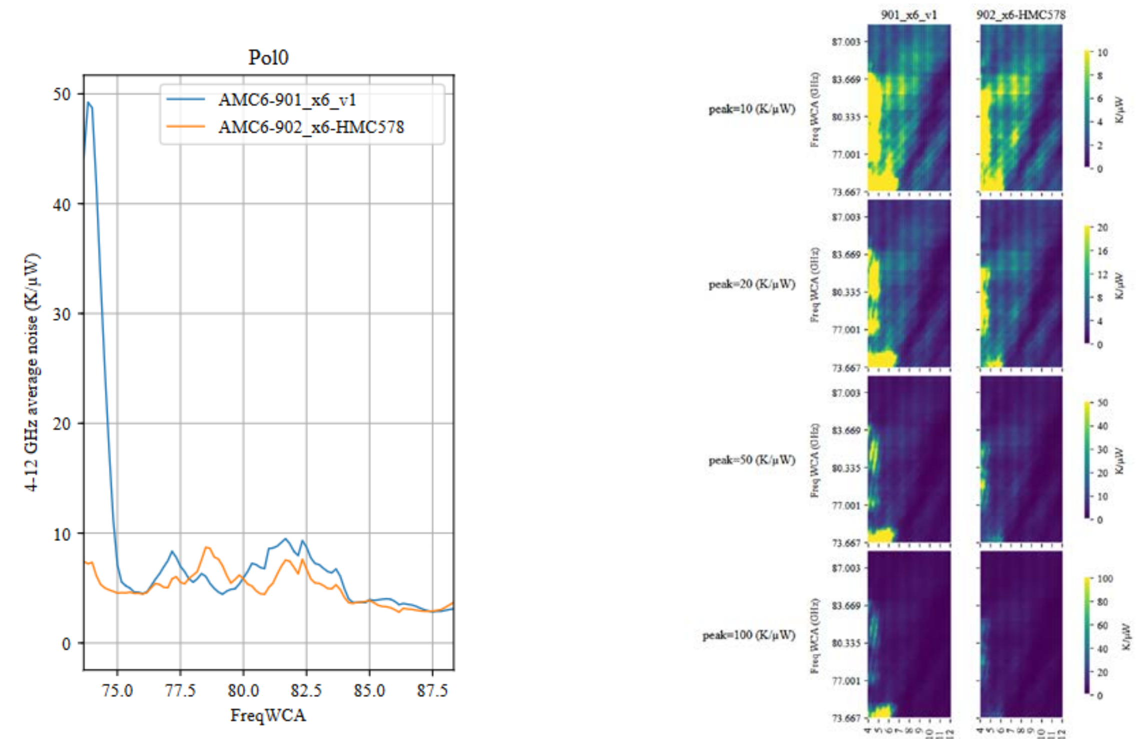

Data Reference: NAFELO-4540

Figure 19: (Left) Comparison of the averaged (over 4 – 12 GHz offset from the carrier) AM sideband noise of a standard AMC6-901 versus that of AMC6-902 incorporating the, alternate, better matched doubler stage. (Right) Variously scaled heatmap data, showing the same comparison in terms of spectral components at 4 – 12 GHz offsets from the carrier. The large amount of AM sideband noise present at 4 – 6 GHz offset from the LO carrier at 73.7 GHz in the original design (primary non-compliance with the average noise specification of 10 K/μW) is significantly reduced, while the noise near 82 GHz LO (already compliant with the averaged specification for the original AMC6 design), remains about the same in the case of the alternate design.

4.4.2 Modified AMC with ×3 architecture

As explained earlier, for this AMC architecture, the input to the AMC would be in the 24 – 30 GHz range, and consequently, the input coaxial-to-microstrip transition design needs to cover the extended frequency range in order to avoid degrading performance due to mismatches between the YTO and the AMC block.

The existing input transition design was analyzed using the CST 3D electromagnetic solver, and the predicted performance is shown in Figure 20.

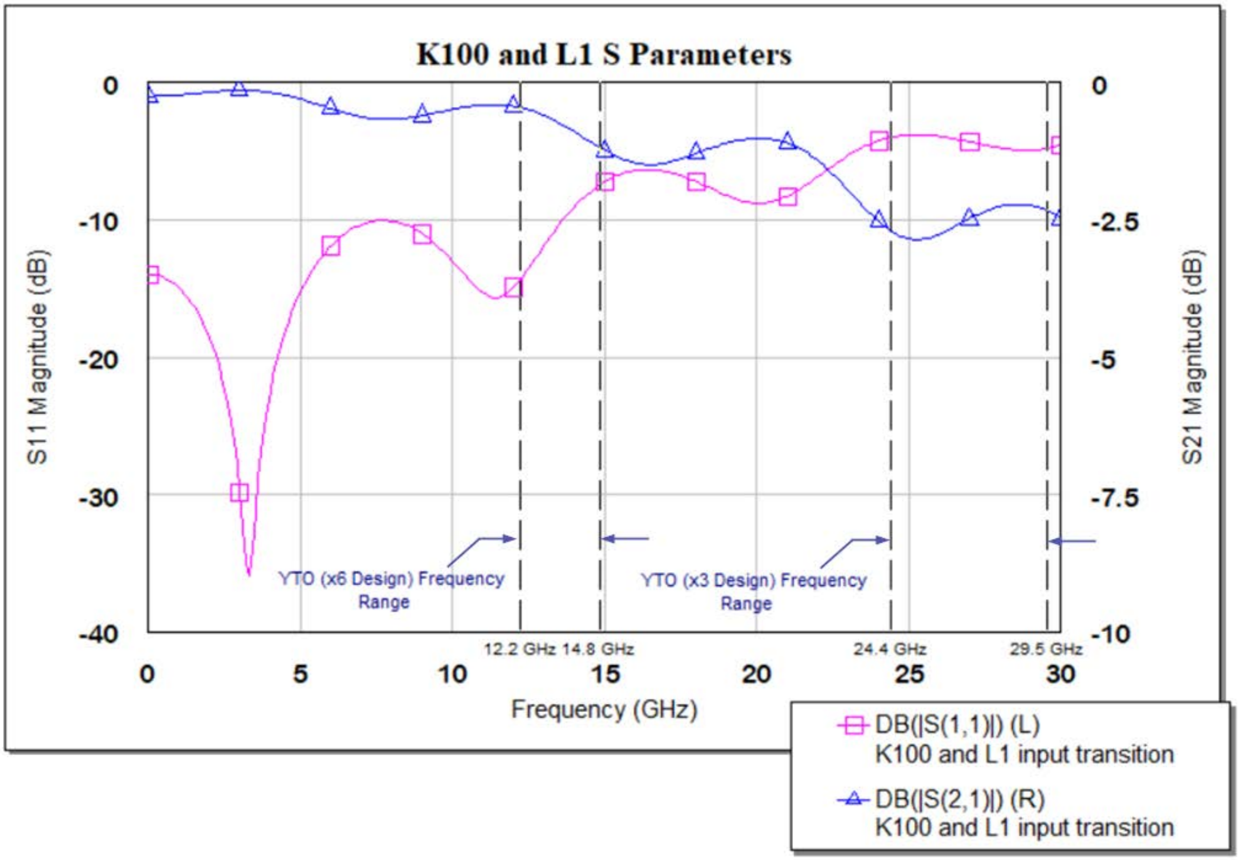

Figure 20: Simulated performance of the input transition used in the existing AMC6 design.

The diameter of the K100 pin is significantly larger than the width of the 50 Ω microstrip line on the 3.5-mil thick alumina substrate used for this design. This was thought to be a significant contributor to the poor return loss of the transition, particularly at higher frequency. To remedy the situation, the revised design utilizes a quartz substrate, which results in a wider 50 Ω microstrip line and yields an improved high frequency performance. The simulated performance of the new transition is shown in Figure 21.

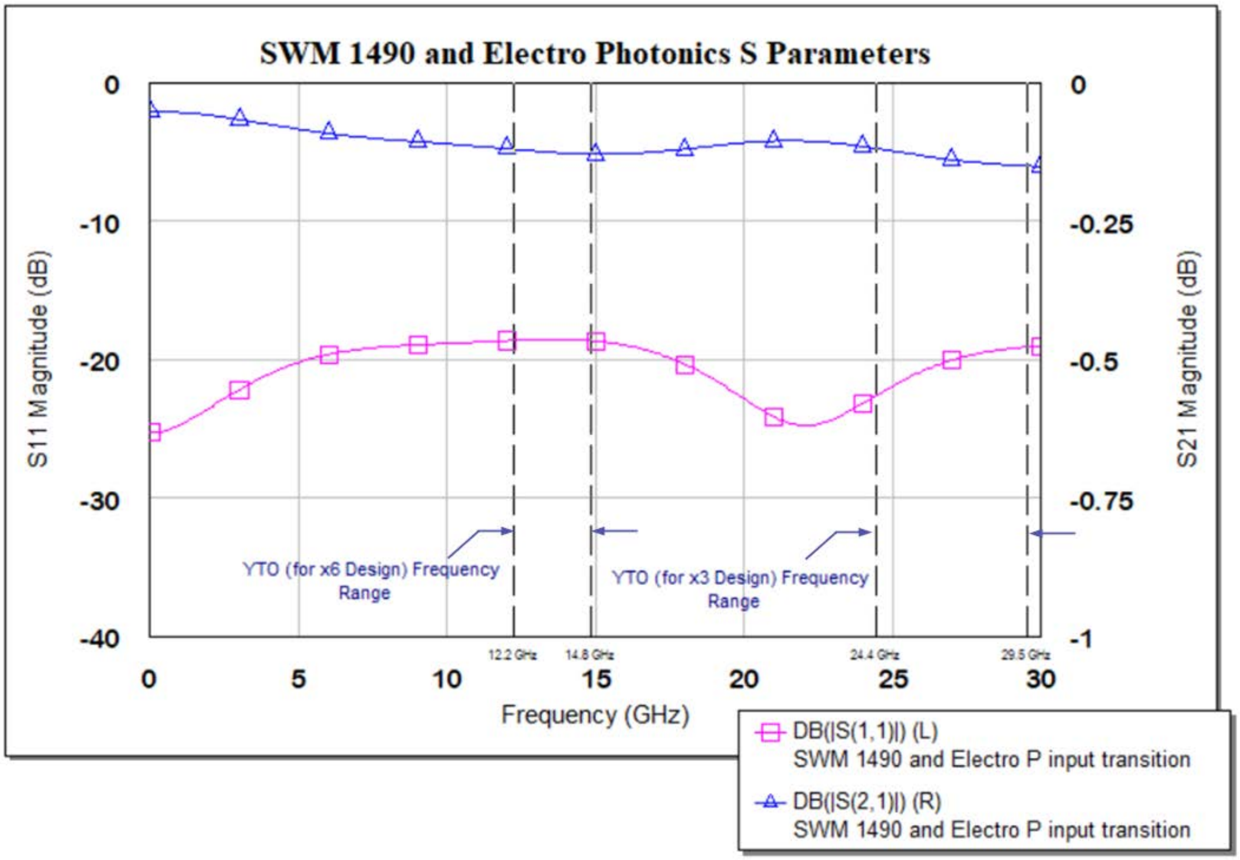

Figure 21: Simulated performance of the quartz-based input transition, designed for the ×3 AMC architecture.

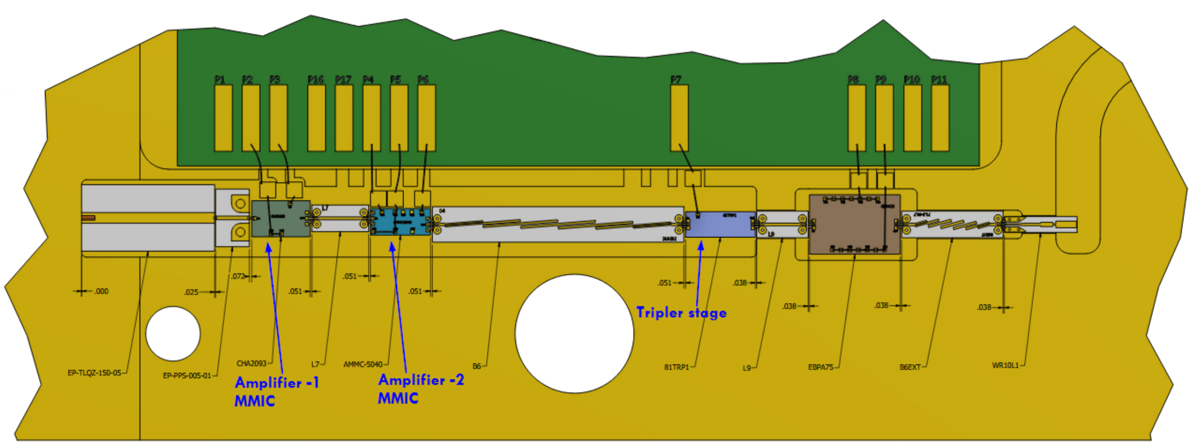

Figure 22: Modified AMC "modv2" block for implementing the proposed ×3 architecture. Compared to a standard AMC6 design, note the wider input transmission line on quartz substrate (instead of alumina) and the missing doubler stage. The rest of the components are preserved, and the extra spaces are bridged using 50 Ω lines.

The AM sideband noise performance of this ×3 architecture AMC was measured and Figure 23 provides a comparison of these results to that of a standard AMC6 performance. The large amount of AM sideband noise present at 4 – 6 GHz offset from the LO carrier at 73.7 GHz in the original design (primary non-compliance with the average noise specification of 10 K/µW) as well as that near 82 GHz LO are both significantly reduced.

The above results corroborate the hypothesis that the input doubler and the adjacent components in the original AMC6 design are the root cause behind the generation of the noise sidebands and the resulting poor AM noise performance of the local oscillator. These results also validate the ability of the ×3 architecture in meeting the AM sideband noise goals while simultaneously placing the lowest fundamental YTO frequency above 20 GHz, thereby making the LO scheme compatible with the wider bandwidth receiver IF goals specified by the ALMA2030 roadmap [RD7] document.

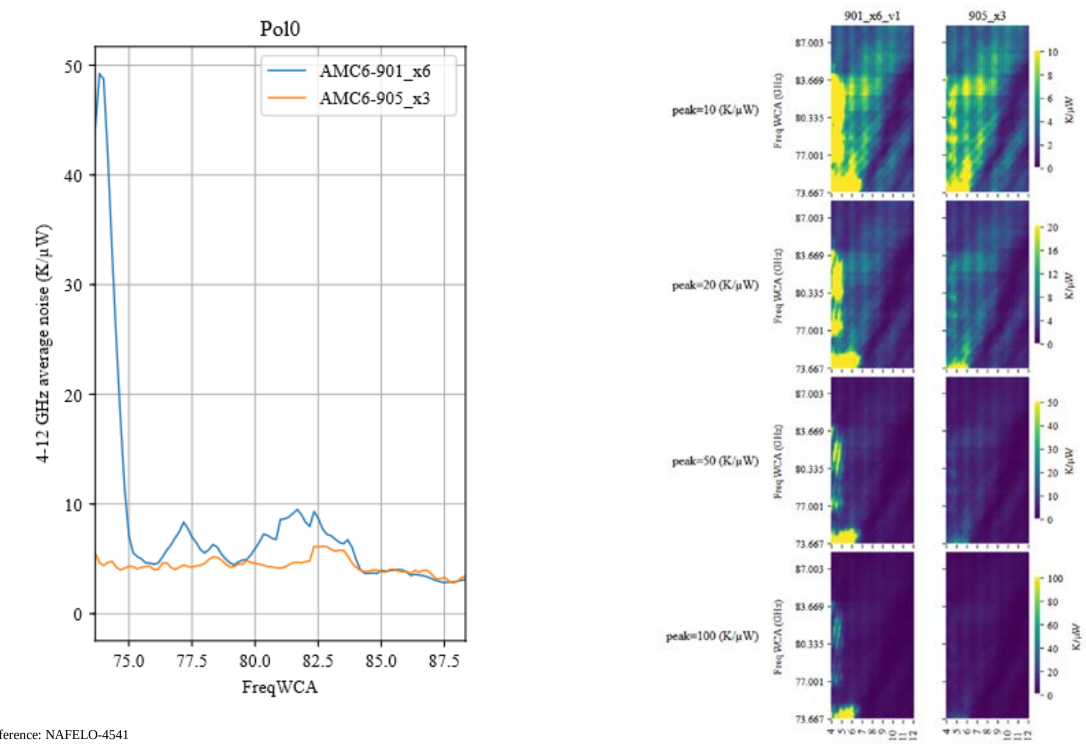

Data Reference: NAFELO-4541

Figure 23: (Left) Comparison of the averaged (over 4 – 12 GHz offset from the carrier) AM sideband noise of a standard AMC6-901 versus that of another AMC6-905 implementing the ×3 architecture. (Right) Variously scaled heatmap data, showing the same comparison in terms of spectral components at 4 – 12 GHz offsets from the carrier. The large amount of AM sideband noise present at 4 – 6 GHz offset from the LO carrier at 73.7 GHz in the original design (primary non-compliance with the averaged noise specification of 10 K/µW) as well as that near 82 GHz LO are both significantly reduced.

4.5 Evaluation of other modifications

Several additional AMC variations were mooted as a result of the test results described in the prior sections. These AMC variants and their measured performances are described in this section.

4.5.1 Standard ×2×3 configuration with improved (quartz-based) input transition

From the results of evaluating an AMC configured with an alternative HMC578 doubler stage (described in section 4.4.1), it was hypothesized that the reflections from the input mismatch of the original HMC331 might be encountering another mismatch on the input side, thereby creating the conditions favorable for generation of noise sidebands at certain frequencies. The junction between the fairly thick K100 pin and the relatively narrow 50 Ω transmission line on the alumina substrate was suspected (although the 50 Ω track is arbitrarily tapered and widened near the junction in the existing AMC6 design in an attempt to ameliorate the suspected discontinuity). Given that the 50 Ω transmission line on the quartz substrate (designed to accommodate the higher input/drive frequency for evaluation of the ×3 AMC configuration described in section 4.4.2) is significantly wider, it was postulated that the noise performance of a standard AMC6 modified with the new quartz substrate at its input would likely result in an improved noise performance even when using the original HMC331 doubler with its poor input return loss. The reasoning being that doing so would remove one of the two mismatches necessary to set up the noise generation/enhancement mechanism.

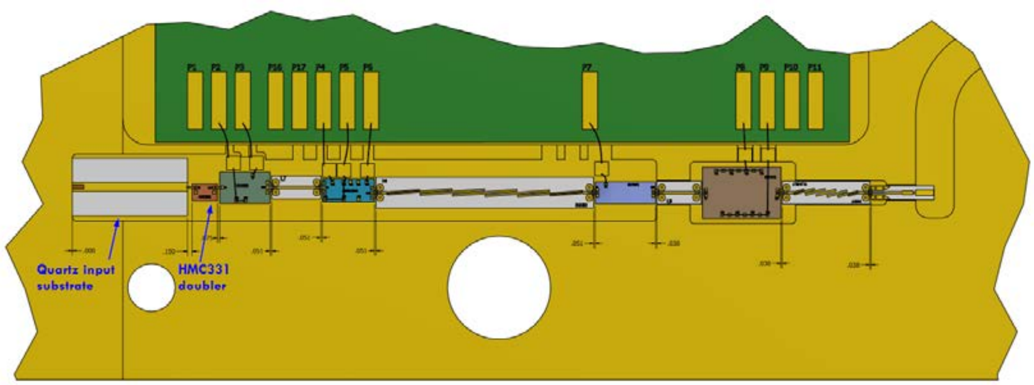

Figure 24:An AMC assembled in the modified AMC "modv2" block, implementing a standard ×2×3 architecture using the original HMC331 doubler. Only the input alumina substrate (50 Ω transmission line) is substituted with an equivalent quartz substrate, all of the other components incorporated are as per the original/standard AMC6 design. Note the wider input transmission line on the quartz substrate (instead of alumina). The increased width of the quartz substrate necessitated the use of the "modv2" block with a wider channel.

Two instances of the AMC implementing the configuration described in Figure 24 were constructed and tested, and yielded the expected improvement in AM sideband noise performance.

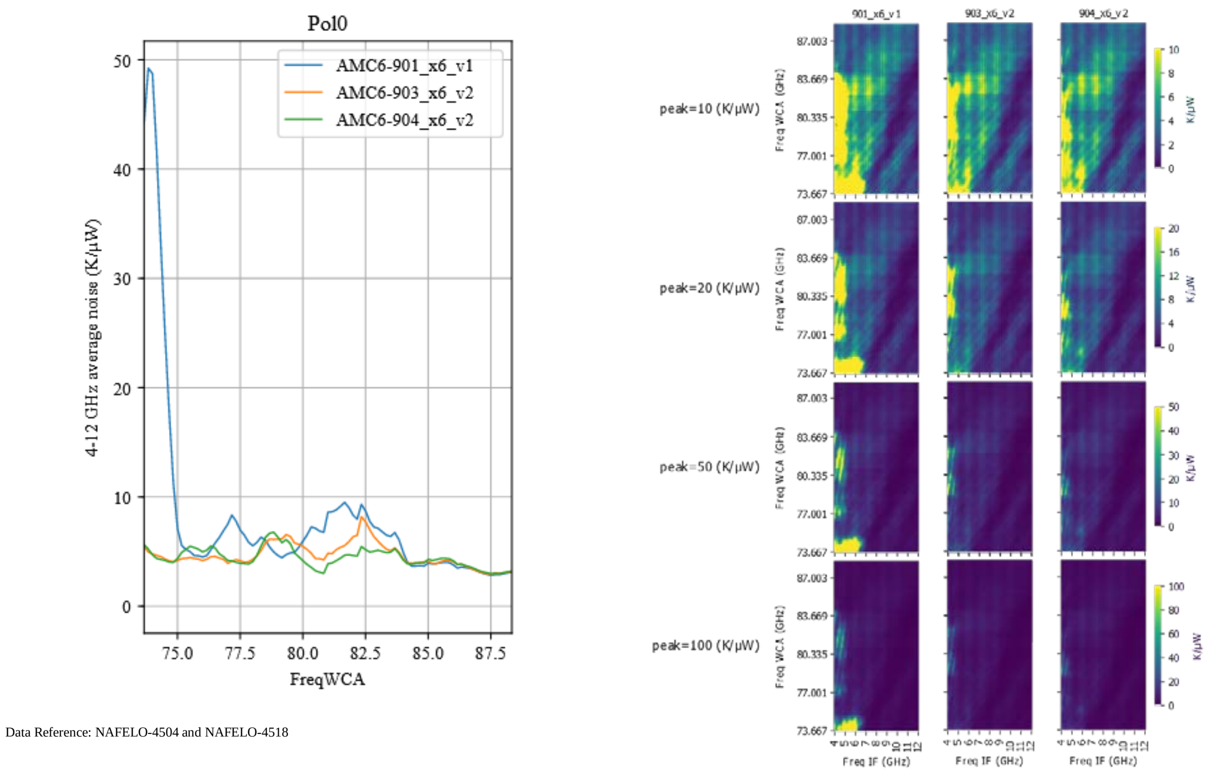

Figure 25: (Left) Comparison of the averaged (over 4 – 12 GHz offset from the carrier) AM sideband noise of a standard AMC6 versus that of the modified AMC with the revised input transition. (Right) Variously scaled heatmap data, showing the same comparison in terms of spectral components at 4 – 12 GHz offsets from the carrier. The large amount of AM sideband noise present at 4 – 6 GHz offset from the LO carrier at 73.7 GHz in the original design (primary non-compliance with the averaged noise specification of 10 K/μW) as well as that near 82 GHz LO are both significantly reduced.

These results corroborate the hypothesis postulated earlier in this section, and represent a possible cost-effective pathway to upgrading all of the existing AMC6s fielded on the ALMA telescope without having to replace them altogether with ones of a new design, and without requiring a new higher frequency YTO. Note that such an AMC upgrade would also not require replacement of a large number of MMICs and/or other components within the existing AMC6s.

4.5.2 Modified AMC with alternate doubler stage (HMC578) and improved (quartz-based) input transition

This AMC variant combines the modifications of the AMC implementation evaluated in section 4.4.1 (with alternate HMC578 doubler) and section 4.5.1 (with improved input transition). Although no further significant improvement over the prior results was expected, this still served as a confirmatory test and also served to affirm the repeatability of the performance improvements resulting from the changes.

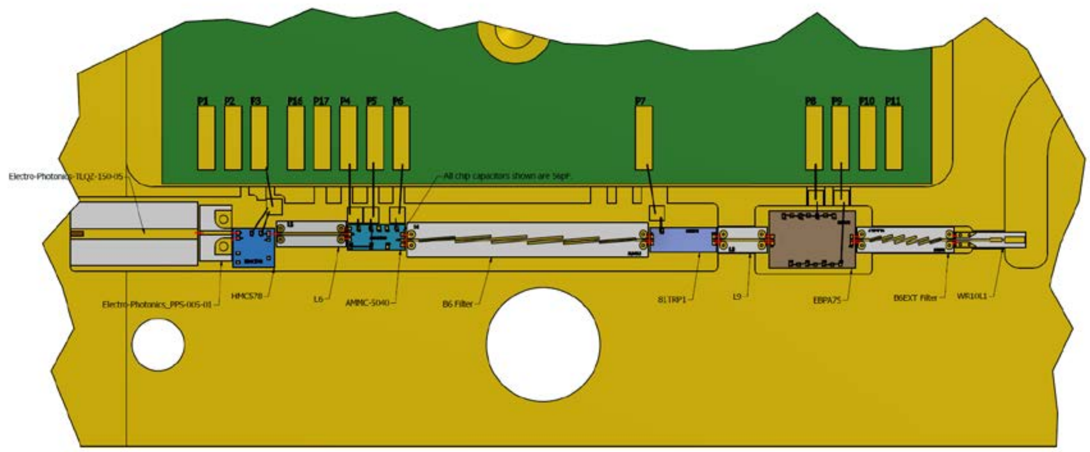

Figure 26: An AMC assembled in the modified AMC "modv2" block, implementing a ×2×3 architecture using the HMC578 doubler. Additionally, the input alumina substrate (50 Ω transmission line) is substituted with an equivalent quartz substrate, all of the other components incorporated are as per the original/standard AMC6 design. Note the wider input transmission line on the quartz substrate (instead of alumina). The increased width of the quartz substrate necessitated the use of the "modv2" block with a wider channel.

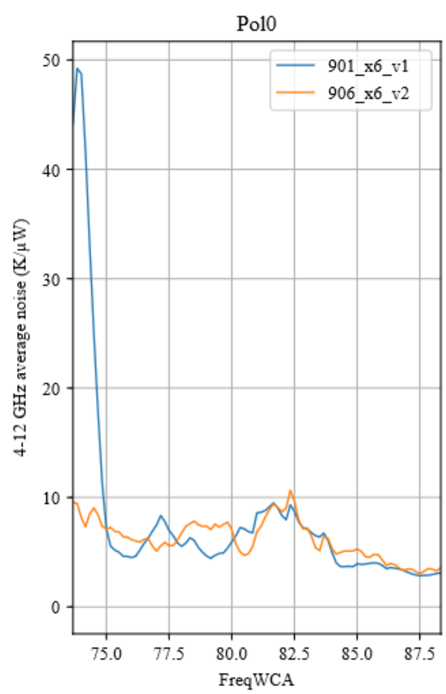

Data Reference: NAFELO-4562

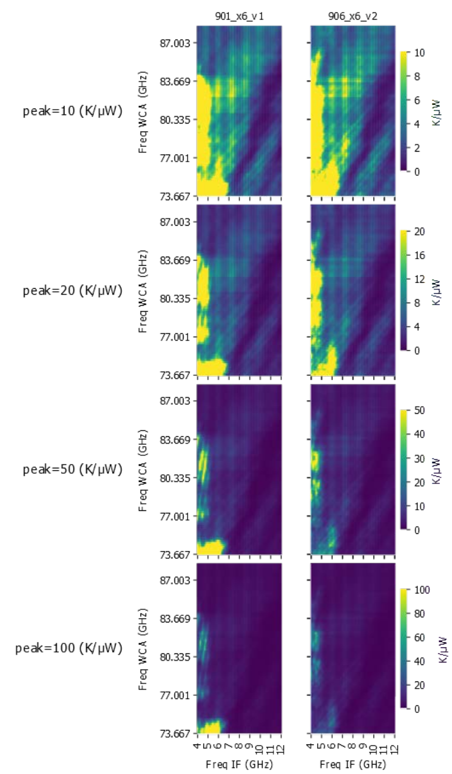

Figure 27: (Left) Comparison of the averaged (over 4 – 12 GHz offset from the carrier) AM sideband noise of a standard AMC6 versus that of another one with the modified input transition and incorporating the HMC578 doubler stage. (Right) Variously scaled data, showing the same comparison in terms of spectral components at 4- 12 GHz offsets from the carrier. The large amount of AM sideband noise present at 4 – 6 GHz offset from the LO carrier at 73.7 GHz in the original design (primary non-compliance with the averaged noise specification of 10 K/μW) is significantly reduced. The noise peak near 82 GHz LO is mostly unchanged.

5 Summary and conclusions

A survey of the experimental results from the evaluation of various AMC architectures and variations described in sections 4.4 and 4.5 indicates that there are several configurations that result in an improved performance and yield results that are compliant with the 10 K/µW AM sideband noise requirement. The following sections describe the relative merits and demerits of each approach and provide the comparative cost estimates for their implementation and roll-out on the ALMA telescope. These considerations are the primary outcome of this ALMA study, and should serve to inform an eventual future decision with regard to the optimal approach for a future retrofit/construction project to implement the Band 6 Front-End LO upgrade in order to meet the ALMA2030 roadmap goals.

5.1 ALMA Band 6 LO upgrade path recommendations

The AMC configurations with an alternate doubler stage (section 4.4.1), improved input transition (section 4.5.1), or both (section 4.5.2) could, in principle, be executed my modifying the existing AMCs and consequently represent the least expensive and the fastest options available to upgrading the Band 6 Front-End LO.

However, they retain the existing ×2×3 AMC architecture which has disadvantages when used with the potential Band 6v2 receiver upgrades which will need to extend the IF range from 4 – 12 GHz to 4 – 16 GHz or more.

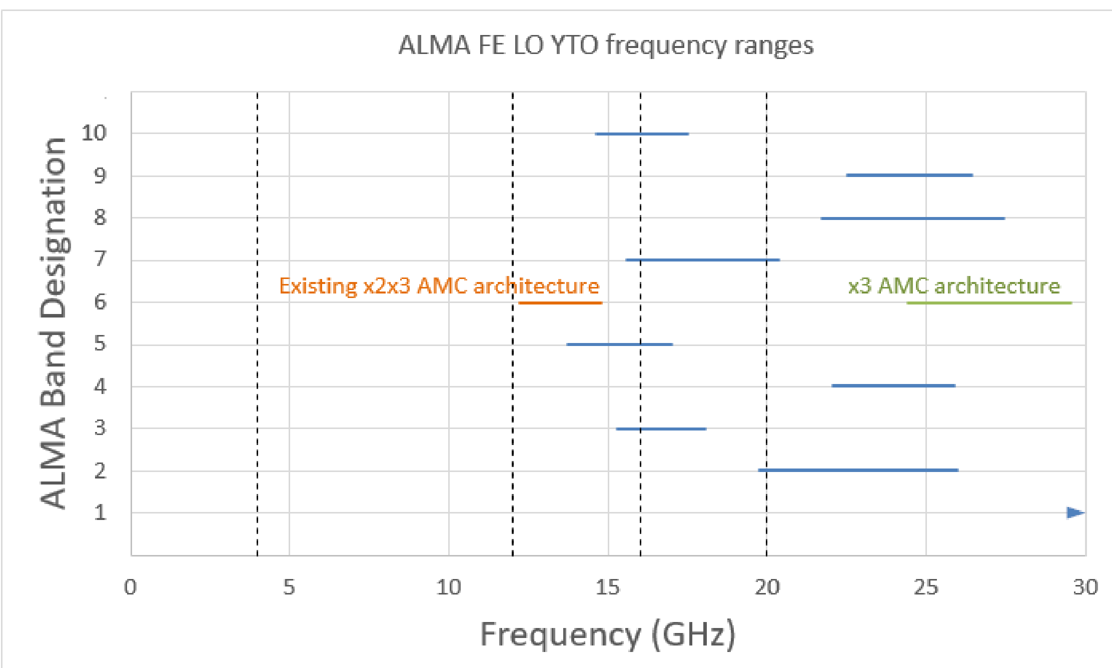

Figure 28: Plot showing the ALMA FE LO YTO frequency ranges (horizontal lines) with respect to the IF ranges of 4 – 12 GHz, 4 – 16 GHz, and 4 – 20GHz (vertical dashed lines). Note that the existing YTO for Band 6 would fall within any extended IF range above 12 GHz. This problem could be alleviated by implementing the alternative ×3 Band 6 AMC architecture. Note also that YTOs for all other bands could, in principle, be parked above 16 GHz when in standby mode, and not interfere with an operational Band 6v2 with an IF up to 16 GHz.

Figure 28 shows the ALMA FE LO YTO frequency ranges with the IF ranges of 4 – 12 GHz, 4 – 16 GHz, and 4 – 20 GHz superposed. Note that the required YTO range for Band 6 using the existing ×2×3 AMC architecture would fall within any extended IF range above 12 GHz. This problem could be alleviated by implementing the alternative ×3 Band 6 AMC architecture described in section 4.4.2. The YTOs for all other bands could, in principle, be parked above 16 GHz when in standby mode, and therefore, would not interfere with an operational Band 6v2 with an IF up to 16 GHz. However, such an approach would require manufacture of a new AMC assembly, and also need a new higher frequency YTO for each antenna/receiver. Consequently, this approach, although technically more attractive, represents the higher cost alternative to the ALMA 2030 Band 6 LO upgrade. Nevertheless, this path is recommended since in addition to getting the new Band 6v2 YTO frequency span out of the extended IF range for Band 6v2, it also alleviates potential future problems of this nature for other ALMA bands when they are upgraded for larger IF ranges as well.

During an upgrade process, Band 6 LO assemblies based on the older and newer architectures could co-exist in any given sub-array since the proposed modification does not have any impact on the photonic reference frequencies required to achieve phase-lock. Tracking of older and newer version hardware will be required to select the appropriate PLL loop bandwidths to ensure fast lock-up and good phase noise performance, but these issues are expected to be dealt with programmatically and with the use of appropriate configuration parameters, and so do not represent any significant implementational challenges.

6 Future work

The sideband AM noise improvements of the promising configurations reported in this study were based on measurements carried out using the LO noise screening test set described in [RD2]. These noise improvements need to be further confirmed and validated with measurements made with actual Band 6 receiver cold cartridges. Although such a task is formally beyond the scope of this study, it is planned to use the prototype parts built and/or procured under this study to construct experimental WCAs that could be used for such a validation effort. Those will be delivered to the Band 6 cold cartridge development team, and serve to carry out such confirmatory tests and inform the decision/choice of the LO configuration selected for a follow-up construction/upgrade project. Towards that goal, at the time of writing this report, a Band 6 WCA6-83 incorporating a ×2×3 configuration AMC with improved (quartz-based) input transition (described in section 4.5.1) has been built and tested and exhibits the expected improved noise performance with respect to the older WCAs, as indicated on Figure 29. Construction of a WCA incorporating the ×3 configuration AMC is currently ongoing.

Additionally, since the ALMA2030 guidelines imply increased IF bandwidth from the present 4 – 12 GHz, to 4 – 16 GHz (at least), the LO AM sideband noise measurements need to be made over correspondingly increased offsets from the LO carrier. This will require revision of laboratory test sets used for noise characterization and remain a topic of interest for future investigation.

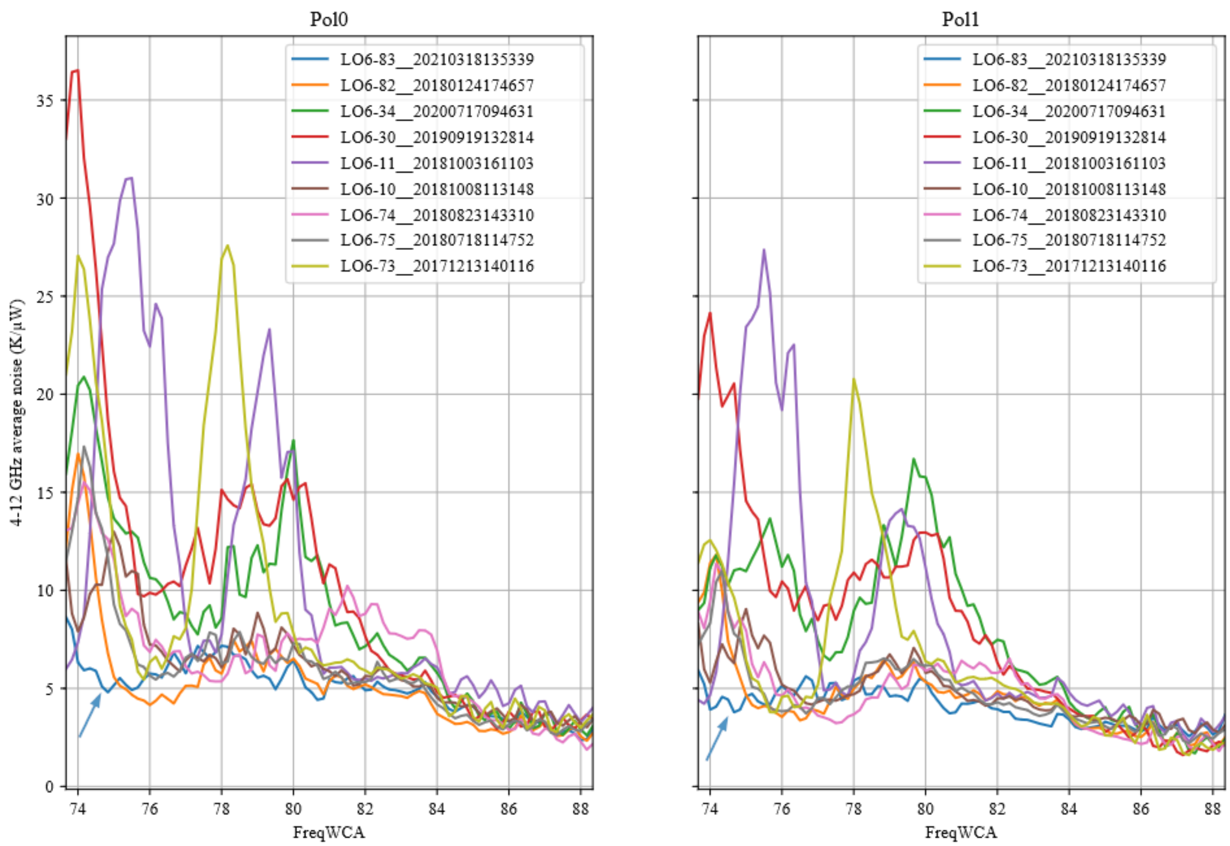

Data Reference: NAFELO-4568

Figure 29: A prototype WCA6-83 incorporating a ×2×3 configuration AMC with improved (quartz-based) input transition (described in section 4.5.1) exhibits the expected improved noise performance with respect to the older/standard WCA6s. Averaged (over 4-12 GHz offset from the carrier) AM sideband noise values are shown in the above comparison plot. An end-to-end receiver noise performance evaluation, in conjunction with a Band 6 cold cartridge assembly, is planned in the future.

7 ALMA Band 6 LO upgrade path schedules and cost estimates

Any upgrade to the ALMA Band 6 LO will require removal of existing Band 6 WCAs on the telescope and their return to the NRAO/CDL for refurbishment. To keep Band 6 operational on the telescopes, this will necessitate the use of spare WCAs (or upgraded WCAs when they arrive). In order to maintain a healthy supply of spares to address any failures, this will necessitate construction of a few brand new WCAs to help start the initial replacement process.

Once the old WCAs are received for upgrades, one of the following will have to be carried out depending upon whether the ×3 or the ×2×3 architecture is desired:

- WCA with ×3 AMC configuration: The old AMC would be replaced with a new AMC. In addition, the old YTO would have to be replaced with a higher frequency YTO. Finally, the modified WCA would need to be fully qualified and returned to the OSF.
- WCA with ×2×3 AMC configuration: The old AMC would need to be removed, refurbished to the new standards, reinstalled into the WCA, and the modified WCA fully qualified and returned to the OSF.

The cost of executing these two options has been estimated and is presented in the following paragraphs and should serve to provide another piece of information for the down-selection/decision-making process. Furthermore, to ensure continuity of ALMA Band 6 receiver operations during the upgrade interval, it is assumed that there shall be a need to first build ten new WCAs of the selected configuration, which will then enable the older ones to be removed and returned for refurbishment. Subsequently, only a quantity of 63 articles will need to be refurbished in order to provide a full complement of WCAs for the telescope (including spares).

7.1 ×3 AMC architecture-based upgrade

For the WCA upgrades incorporating the ×3 AMC configuration, which is the recommended option, the design reviews were synchronized with the corresponding Band 6v2 cold cartridge reviews as proposed in the recently submitted NA ALMA Cycle 9 development project proposal. The remaining tasks were subsequently scheduled around the PDR and CDR appropriately as shown in Figure 30. The total cost (both direct and indirect) for this work is estimated to be $3.6 M, and the corresponding cost profile is shown in Figure 31.

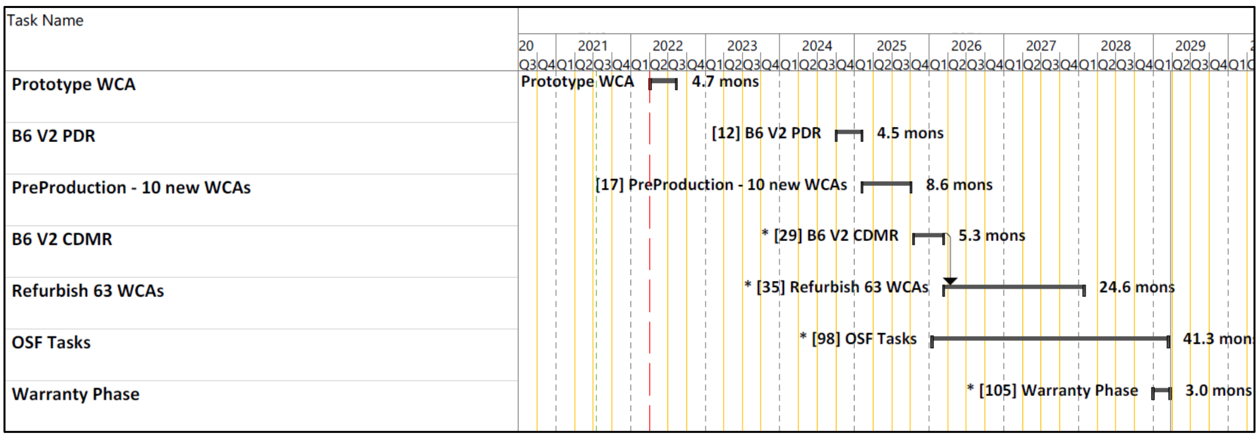

Figure 30: Top level view of the Gantt chart showing the schedule for WCA upgrades (with the ×3 AMC configuration). The design reviews were synchronized with the corresponding Band 6v2 cold cartridge reviews as proposed in the recently submitted NA ALMA Cycle 9 development project proposal. The corresponding cost profile is shown in Figure 31.

.

	FY2022	FY2023	FY2024	FY2025	FY2026	FY2027	FY2028
Labor	$112,122	$238,352	$138,454	$128,577	$0	$25,258	$16,529
ME&S	$187,776	$267,088	$225,959	$1,060,650	$201,991	$162,683	$166,578
Travel	$0	$0	$0	$0	$0	$0	$0
Indirect Costs	$54,163	$126,125	$79,030	$338,653	$14,483	$8,263	$5,407
Total	**$354,060**	**$631,566**	**$443,442**	**$1,527,880**	**$216,474**	**$196,205**	**$188,514**

Figure 31: Projected cost-profile for the work shown in the Gantt-chart of Figure 30 to upgrade all the Band 6 LO systems with WCAs incorporating the ×3 architecture option. The grand total of all of the indicated yearly amounts is $3.6M.

7.2 ×2×3 AMC architecture-based upgrade

For the case of WCA upgrades while retaining the ×2×3 AMC configuration, which is the lower cost option that could be implemented to improve the noise performance of the existing Band 6 receivers on the ALMA telescope, Figure 32 depicts a possible schedule with a CDMR after the initial build of ten new WCA articles, and then, immediately followed by the refurbishment of 63 articles. The total cost (both direct and indirect) for this work is estimated to be 860 k$, and the corresponding cost profile is shown in Figure 33.

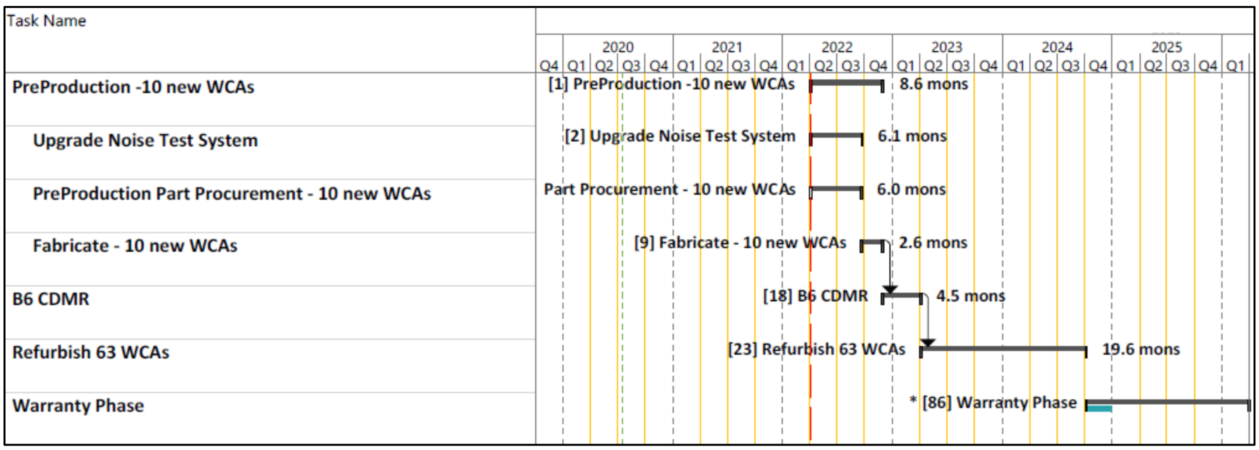

Figure 32:Top level view of the Gantt chart showing the schedule for WCA upgrades (with the ×2×3 AMC configuration). The schedule assumes a CDMR after the initial build of ten new WCA articles, and then, immediately followed by the refurbishment of 63 articles. The corresponding cost profile is shown in Figure 33.

	FY2022	FY2023	FY2024	FY2025
Labor	$69,319	$155,186	$43,322	$23,808
Material & Services	$263,302	$29,755	$48,958	$0
Travel	$0	$0	$0	$0
Equipment > $5000	$18,750	$0	$0	$0
Indirect Costs	$108,819	$60,504	$30,190	$7,789
Total	**$460,190**	**$245,445**	**$122,470**	**$31,597**

Figure 33: Projected cost-profile for the work shown in the Gantt-chart of Figure 32 to upgrade all the Band 6 LO systems with WCAs incorporating the ×2×3 architecture option. The grand total of all of the indicated yearly amounts is 860 k$.

8 Programmatic notes

8.1 Schedule performance

This ALMA Band 6 LO modifications study was predominately experiment based and consequently, its schedule was negatively impacted by the pandemic related shutdown and work slow-down which occurred during the April-August 2020 operating period. Work on design tasks that were possible to be carried out remotely did continue, but progress continued to be hampered by restricted access to the laboratories. Close to the original finish-by date of 9/30/2020, this project was at approximately 50% completion. Consequently, a 6-month no-cost extension [RD9] was sought (and granted) for this 1-year duration project, and the remaining work was successfully completed during this additional period.

8.2 Budget performance

As expected, due to the slow-down, the actual expenditure rate lagged behind the planned spend rates, but overall, the budget was sufficient to complete the scope of the effort over 1.5 years. At the end of the project, about 11% of the funds remained unspent.

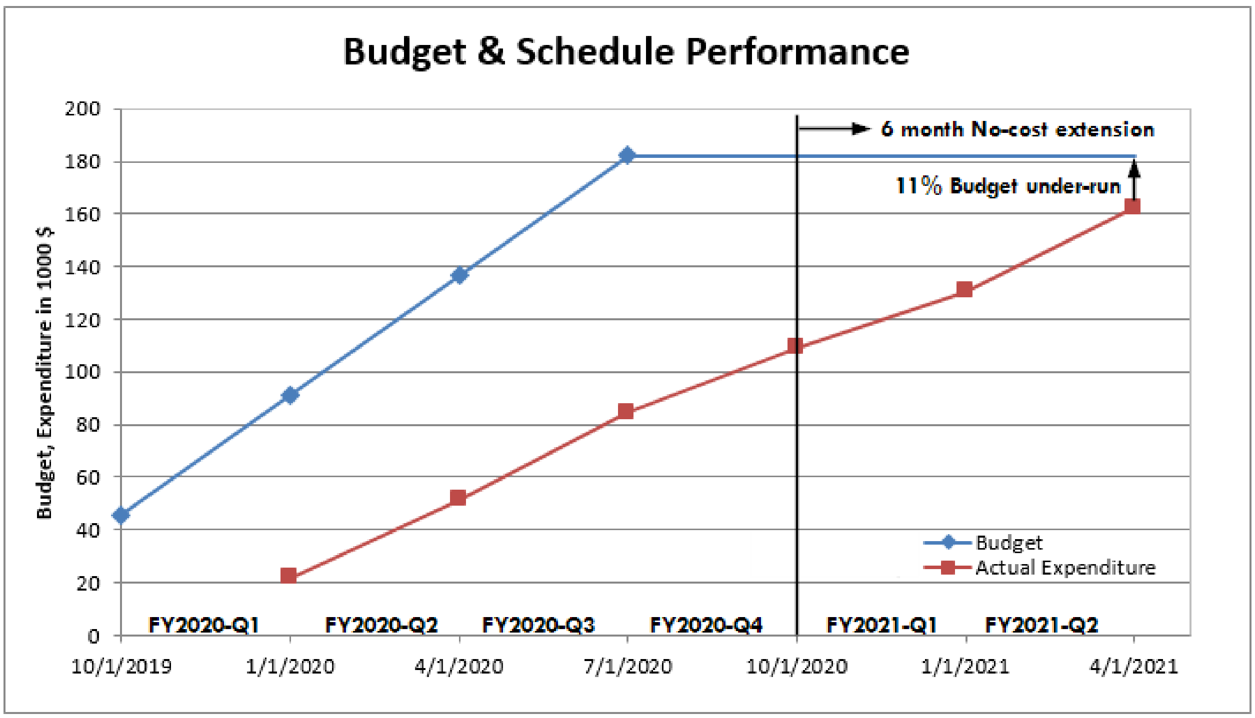

Figure 34: Schedule and budget performance for the NA ALMA Development Cycle 7 study, titled, "ALMA Band 6 Local Oscillator Modifications."

8.3 Co-op student participation

This study provided the platform for a co-op student to work on the analysis, assembly/construction, and laboratory testing of a millimeter-wave device for a real-world telescope sub-system, and be mentored by the study principal investigators. Funding for the co-op student was not covered by the study allocations, but that effort was an in-kind contribution from NRAO/CDL to this ALMA development study.

9 Reference Documents

[RD1] K. Saini and D. Vaselaar, "Cycle 7 NRAO ALMA Development Study Proposal – ALMA Band 6 Local Oscillator Modifications," submitted on 26th April 2019.
Public Abstract available at https://science.nrao.edu/facilities/alma/alma-develop-old-022217/Saini.pdf
Full Proposal available at https://sharepoint.nrao.edu/pmd/Proposal Files/651 ALMA Band 6 LO Modifications/651 ALMA Band 6 LO Modifications - ALMA-D Study Proposal.pdf?Web=1

[RD2] E. Bryerton, "AM Noise in Front End Local Oscillators," FEND-40.10.00.00-093-F-REP, Version F, 21st August 2013.
Available at http://edm.alma.cl/forums/alma/dispatch.cgi/iptfedocs/docProfile/105209

[RD3] N. Whyborn, B. Lopez, et. al., "Band 6 Version 2 Conceptual Design Review (CoDR) Review Panel Report," ALMA-40.02.06.00-1037-A-REP, Version A, 22nd October, 2018.
Available at https://sharepoint.nrao.edu/pmd/_layouts/15/WopiFrame2.aspx?sourcedoc=/pmd/Proposal Files/651 ALMA Band 6 LO Modifications/651 ALMA Band 6 LO Modifications - ALMA-D Study Proposal.pdf&action=default

[RD4] M. Mereles, "Band 6 AMC Frequency Tripler Performance," 12th October, 2019.
Available at https://sharepoint.nrao.edu/cdl/_layouts/15/WopiFrame.aspx?sourcedoc=/cdl/Shared Documents/ALMA/Cy.7 Band 6 LO Study/Reports and Summaries/81TRP1_Tb/tripler_test_block_testing_report.docx&action=default

[RD5] Analog Devices, "GaAs MMIC Passive Frequency Doubler, 12 – 18 GHz Input," Obsolete datasheet available at https://www.analog.com/media/en/technical-documentation/data-sheets/hmc331.pdf

[RD6] Analog Devices, "GaAs MMIC x2 Active Frequency Multiplier, 24 – 33 GHz Output," Die datasheet available at https://www.analog.com/media/en/technical-documentation/data-sheets/hmc578chips.pdf

[RD7] J. Carpenter, D. Iono, L. Testi, N. Whyborn, A. Wootten, N. Evans (The ALMA Development Working Group), "The ALMA Development Roadmap," 12th July, 2018.
Available at https://www.almaobservatory.org/wp-content/uploads/2018/07/20180712-alma-development-roadmap.pdf

[RD8] S. Asayama, G. H. Tan, K. Saini, et. al., "Report of the ALMA Front-end & Digitizer Requirements Upgrade Working Group," ALMA-05.00.00.00-0048-A-REP, Version B, 16th December, 2020.

[RD9] K. Saini, "Change Request for 651 ALMA Band 6 LO Modifications," NRAO Document No. NRAO-28-10042, 21st August, 2020.
Available at https://sharepoint.nrao.edu/pmd/_layouts/15/WopiFrame2.aspx?sourcedoc=/pmd/Proposal Files/651 ALMA Band 6 LO Modifications/651 ALMA Band 6 LO Mod CR 01.pdf&action=default